# The Interaction Between Credit Constraints and Uncertainty Shocks[†]

Pratiti Chatterjee[a,‡], David Gunawan[⋆], and Robert Kohn[⋆⋆]

January 2021

**Abstract**

We propose a novel link between credit markets and uncertainty shocks. Empirically, we estimate time-varying uncertainty about credit in the U.S. and decompose it into a "pure" (independent) second-moment shock versus a second-moment change that is correlated with a first-moment shock. We show that a pure second-moment shock has almost no effect in expansions, but generates a significant decline across measures of real activity in recessions. To build intuition, we feed our estimated uncertainty process into a flexible-price real business cycle model with collateral constraints. A shock to credit uncertainty triggers a precautionary response that interacts with the collateral constraint to generate a sizable and simultaneous decline in output, consumption, investment, real wages, and hours. This interaction is a novel feature and generates the simultaneous decline in these variables that previous work on uncertainty shocks without credit constraints has been unable to produce in a flexible price environment.

JEL Classification Codes: C32, E32, E44

Keywords: Credit Constraints, Credit Fluctuations, Local Projections, Recessions, Stochastic Volatility, Uncertainty Shocks

[†]We would like to thank Saroj Bhattarai and Eric Swanson for excellent comments and feedback.

[a]Corresponding author. [‡]Level 4, West Lobby, School of Economics, University of New South Wales Business School – Building E-12, Kensington Campus, UNSW Sydney – 2052; *Email:* pratiti.chatterjee@unsw.edu.au, *Phone Number:* (+61) 293852150. Website: `http://www.pratitichatterjee.com`

[⋆]39C. 164, School of Mathematics and Applied Statistics (SMAS), University of Wollongong, Wollongong, 2522; Australian Center of Excellence for Mathematical and Statistical Frontiers (ACEMS); National Institute for Applied Statistics Research Australia (NIASRA); *Email*: dgunawan@uow.edu.au. *Phone Number:* (+61) 424379015.

[⋆⋆]Level 4, West Lobby, School of Economics, University of New South Wales Business School – Building E-12, Kensington Campus, UNSW Sydney – 2052, and ACEMS *Email:* r.kohn@unsw.edu.au, *Phone Number:* (+61) 424802159.

The research of David Gunawan and Robert Kohn were partially supported by the ARC Center of Excellence grant CE140100049.

# 1 Introduction

The aftermath of the 'Great Recession' witnessed a surge of interest in examining the importance of uncertainty in generating business cycle fluctuations, with an early and important contribution by Bloom (2009). More recently, the COVID-19 pandemic triggered financial market uncertainty - both through changes in measures such as the VIX or uncertainty about access to credit.[1] Concurrently, the role of credit markets in shaping business cycle dynamics has gained traction with many authors documenting a link between credit build up in periods of expansion and the subsequent crash in recessions; e.g., Jordà, Schularick, and Taylor (2013), Mian and Sufi (2018). Our article proposes a novel description of the link between credit markets and uncertainty shocks. We exploit the dynamics of credit expansion and contraction to explicitly pin down the role of uncertainty shocks in credit markets to quantify how a change in the second moment transmits into the real economy.

We begin by presenting a new stylized fact that stems from the time-variation in the volatility of credit expansions and contractions. These changes are interpreted as time-variations in credit-uncertainty and a stochastic volatility model is estimated to document that time-varying uncertainty in credit dynamics is a robust empirical feature. Our approach to estimating the stochastic volatility model is based on recent advances in Bayesian methodology for state space models. In particular, we use the correlated version of pseudo marginal Metropolis-Hasting (PMMH) proposed by Deligiannidis et al. (2018) that is more efficient in comparison existing methods. We incorporate the empirically identified uncertainty in credit dynamics in a flexible price real business cycle model with a collateral constraint on firm borrowing. In a parsimonious environment, we show that unforeseen changes in credit-uncertainty interacts with the borrowing constraint distortion to generate significant changes in real activity. This interaction between credit constraints and precautionary motives is a novel feature that helps forge a direct link between the source and manifestation of uncertainty in the real economy.

The article makes several important contributions. First, we present a new stylized fact that quantifies credit-uncertainty over the business cycle. We document time-variation in the volatility of credit-growth and credit availability as a robust empirical feature that is consistently observed across different measures of credit aggregates.

Second, we fit a time series model of these shocks and quantify their effects on macroe-

[1]The role of credit market uncertainty in the face of the COVID-19 pandemic has been explicitly addressed in speeches by policy makers across financial institutions across countries. Statements issued by: Board of Governors of the Federal Reserve System: `https://www.federalreserve.gov/newsevents/pressreleases/bcreg20200323a.htm`, Reserve Bank of Australia: `https://www.rba.gov.au/speeches/2020/sp-gov-2020-03-19.html`, Reserve Bank of India: `https://www.rbi.org.in/Scripts/bs_viewcontent.aspx?Id=3847`.

conomic variables. This is done by separating the identified shock into two components – one that captures the 'pure' effect of a change in the second moment that is independent of changes in the first moment, and the other capturing a change in the second moment that is correlated with a shock to the first moment. To quantify the impact of shocks to credit-uncertainty, the extracted shocks are used to construct impulse responses using the local projections method (Jordà, 2005). Impulse responses are constructed for two scenarios: one in a linear model with no distinction between recessions and expansions; the other in a state-dependent version of local projections that allows for differences between recessions and expansions.

For both the linear and state-dependent local projections, we find that the effects of 'pure' shocks to credit-uncertainty are contractionary; in recessions, the effects are significantly larger and with almost no effects in expansions. We show that a shock to credit-uncertainty can generate a slowdown across a broad measure of real activity. During downturns, a one-standard deviation increase in credit-uncertainty triggers a sharp and significant decline in auto-sales, durable goods consumption, and investment. Household leverage declines and the credit spreads increase sharply as well. More broadly, aggregate consumption and GDP contracts; the unemployment rate shows a significant increase a few periods after the shock hits and non-durable consumption declines. To take a deeper look at the response of unemployment we also examine the response of total employed and find a significant decline on impact that lasts several quarters. If the uncertainty shock embeds first moment implications, these effects are even larger. An important takeaway from our results is that shocks to credit-uncertainty in good times *does not* impede the pace of real activity. During busts, however, a shock to the second moment can exacerbate the depth as well as the duration of a recession. We therefore empirically establish this asymmetry in the way the uncertainty shock propagates in the economy.

To build intuition, the estimated uncertainty process is fed to a flexible price real business cycle model with collateral constraints. We show that when the collateral constraint binds, an increase in credit-uncertainty leads to a simultaneous decline in consumption, investment, output, real wages, and hours worked. Using properties of the pruned third-order solution we isolate the precautionary response from the endogenous transmission operating through the higher order interaction terms. In the model, the shock transmits itself by increasing the wedge between labor demand and labor supply. Although labor supply increases through the initial precautionary response of households to the shock, the increase in the wedge operating through the collateral constraint on firm borrowing is strong enough to generate a contraction in labor demand leading to decline in hours and real wages in equilibrium. Thus, even in the absence of other distortions and shocks, an uncertainty shock in our proposed framework can generate a sizable and simultaneous

impact on macroeconomic variables consistent with the stylized facts characterizing the transmission of aggregate uncertainty to the real economy. This is our third main result.

We also consider an extension with hand-to-mouth consumers with no access to saving mechanisms that dilutes the precautionary savings response by households. Despite this feature, we find that changes in credit-uncertainty generates a sizeable decline in macroeconomic variables with a disproportionately larger consumption decline for the hand-to-mouth agents.

*Related Literature:* The first group of studies connected to our paper examine the role of uncertainty in generating business cycle fluctuations. Bloom (2009), Fernández-Villaverde, Guerrón-Quintana, Rubio-Ramírez, and Uribe (2011), Fernández-Villaverde, Guerrón-Quintana, Kuester, and Rubio-Ramírez (2015), Leduc and Liu (2016), Basu and Bundick (2017), Bloom, Floetotto, Jaimovich, Saporta-Eksten, and Terry (2018), Berger, Dew-Becker, and Giglio (2020) and, Fernández-Villaverde and Guerrón-Quintana (forthcoming) among others, motivate the role of shocks to the second moment as a driver of business cycles.[2] Uncertainty in these papers stems from the time-varying volatility in exogenous shocks to aggregate productivity, aggregate demand, fiscal policy, borrowing costs or from a realized volatility perspective. One of the challenges in the theoretical literature examining the effects of uncertainty has been to generate a sizable impact and simultaneous decline in key macro variables (output, hours, consumption and investment). Our approach to modeling uncertainty and its interaction with the real economy thus overcomes the quantitative irrelevance result of time-variation in uncertainty in RBC models that has been described in Fernández-Villaverde and Guerrón-Quintana (forthcoming), and is better able to explain the simultaneous decline in these variables than existing models of uncertainty shocks.

Our work is also related to studies that examine the role of financial conditions in transmitting uncertainty shocks. Caldara, Fuentes-Albero, Gilchrist, and Zakrajšek (2016) use a sequential identification technique, and Alessandri and Mumtaz (2019) distinguish between regimes of financial-stress and financial-calm to explore the role of financial conditions in the transmission of uncertainty. They find that, while uncertainty shocks by themselves can generate business cycle fluctuations, the severity of the impact increases significantly when uncertainty shocks interact with financial conditions. Ludvigson, Ma, and Ng (forthcoming) and Caggiano, Castelnuovo, Delrio, and Kima (2020) using shock-based restrictions find that sharply higher macroeconomic uncertainty in recessions is often an endogenous response to output shocks, while uncertainty about financial markets is a likely source of output fluctuations. Instead of imposing identifying

[2]See Fernández-Villaverde and Guerrón-Quintana (forthcoming), for a detailed review on the literature on uncertainty shocks and business cycle research.

restrictions, and regime dependencies, we construct our measure of uncertainty shocks, from the time-variation in the volatility of credit expansions and contractions, and we show that changes in credit uncertainty can generate a sharp slowdown across a broad measure of real activity in recessions with almost no effects in expansions.

A third related strand of the literature examines the differences between financial and nonfinancial recessions. The importance of credit growth in shaping business cycles has been studied in detail by Jordà, Schularick, and Taylor (2013) who show that the patterns of credit growth can predict the type of recovery with periods of high credit growth being followed by recessions that are deeper and longer. When the real effects of shocks to credit-uncertainty are analyzed, we find that these shocks (independent of changes in the first moment) can exacerbate the depth and duration of a recession by amplifying the slowdown. Our article presents a potential explanation for the heightened depth and duration of recessions following a credit buildup.

Our article is also related to the studies that examine the importance of financial factors during the Great Recession. Jermann and Quadrini (2012) for instance examine the role played by the dynamics of the firms' financing decisions; Christiano, Eichenbaum, and Trabandt (2015) examine the importance of a financial wedge distorting the intertemporal Euler equation for capital accumulation, Christiano, Motto, and Rostagno (2014) and Arellano, Bai, and Kehoe (2019) examine the role of changes in the idiosyncratic productivity of firms.[3] Alfaro, Bloom, and Lin (2019) suggest that the size of the finance uncertainty multiplier is significant and plays an important role in the transmission of uncertainty shocks. Our work provides a complementary view to the role of financial factors by isolating a shock to credit-uncertainty. We quantify the independent effects of a change in the second moment vis-*à*-vis a change the in the first moment and show that shocks to credit-uncertainty by itself can generate a significant slowdown across a broad measure of real activity.

In terms of technique and approach to modeling uncertainty, our paper is related to Fernández-Villaverde, Guerrón-Quintana, Rubio-Ramírez, and Uribe (2011) and Fernández-Villaverde, Guerrón-Quintana, Kuester, and Rubio-Ramírez (2015). Like these papers we use sequential Monte Carlo methods; however, one advantage of our method is that the implementation is more efficient. The remainder of the paper is organized as follows. Section 2 describes the data, modeling and estimation techniques used to uncover time-variation in credit uncertainty. Section 3 discusses the results of the estimation. Section 4 empirically quantifies the real effects of the extracted uncertainty shocks. Section 5 presents a theoretical model to outline the transmission mechanism.

[3]See Gertler and Gilchrist (2018) for a detailed survey on studies examining the role of financial factors during the Great Recession.

Section 6 presents a robustness check of our results. Section 7 concludes.

# 2 Testing the existence of stochastic volatility

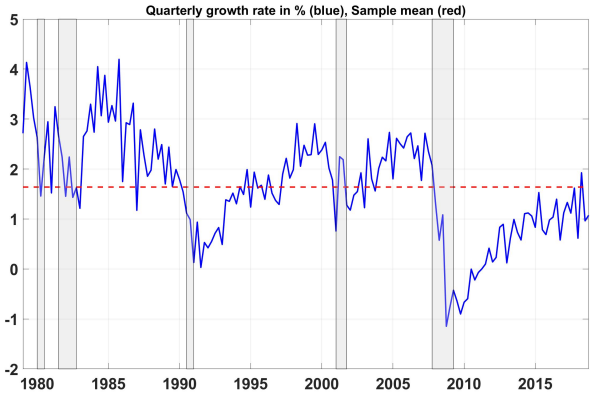


**Figure 1:** Total credit extended to the nonfinancial sectors. Shaded areas indicate NBER recessions.

## 2.1 Data

To examine the presence of time variation in credit-uncertainty we begin by looking at the dynamics of the quarterly change in the growth rate of total credit extended to the private nonfinancial sector in the U.S.. The 'private nonfinancial sector' includes nonfinancial corporations (both private-owned and public-owned), households and non-profit institutions serving households as defined in the System of National Accounts 2008. The series are at quarterly frequency and capture the outstanding amount of credit at market value at the end of the reference quarter. In terms of financial instruments, credit covers loans and debt securities.[4] The estimation sample extends from 1979 Q1 to 2018 Q4; this series is denoted as $y_t$. Figure 1 plots the quarterly growth rate of credit available to the nonfinancial sector. We start our analysis with this broad measure of credit and use this definition when discussing the results in sections 3, 4 and 5. Section 6.3 carries out robustness checks accounting for different measures of credit aggregates and shows that the estimates characterizing credit uncertainty is a robust empirical feature across these different measures.

[4]For more details see credit data on BIS statistics repository. The series source code is Q:US:P:A:M:USD:A.

## 2.2 Empirical Model

Time variation in credit-uncertainty is isolated by considering a stochastic volatility (SV) model for $y_t$ allowing for correlation between shocks to the level and the standard deviation of credit-growth (leverage effect), with observation equation

$$y_t = \phi_y y_{t-1} + \exp\left(h_t/2\right)\epsilon_t, \quad \epsilon_t \sim N\left(0,1\right), \quad t = 1,2,...,T; \tag{1}$$

$\epsilon_t$ is a standard normal random variable. The important feature of the model is that the log-volatility $h_t$ is not constant, but follows the AR(1) process,

$$h_{t+1} = \overline{\mu_h} + \phi_h\left(h_t - \overline{\mu_h}\right) + \tau\eta_{t+1}, \quad \eta_{t+1} \sim N\left(0,1\right), \quad t \geq 1; \tag{2}$$

$$\begin{pmatrix} \epsilon_t \\ \eta_{t+1} \end{pmatrix} \sim N\left(\begin{pmatrix} 0 \\ 0 \end{pmatrix}, \begin{pmatrix} 1 & \rho \\ \rho & 1 \end{pmatrix}\right); \tag{3}$$

$\eta_t$ is normally distributed with mean zero and unit variance. The parameters $\overline{\mu_h}$ and $\tau$ control the degree of mean volatility and stochastic volatility in $y_t$, respectively. The process $\{y_t\}$ is hit by both $\epsilon_t$ and $\eta_t$; the innovation $\epsilon_t$ to the observation $y_t$ changes the level of $y_t$; the innovation $\eta_t$ to the volatility of $y_t$ affects the standard deviation of $\epsilon_t$. When estimating the model, the data is demeaned. The parameter $\rho$ controls the strength of the dependence between $\epsilon_t$ and $\eta_t$ – the size of the "leverage effect" of the level shock $\epsilon_t$ on the volatility shock $\eta_t$. Uncertainty shocks in this environment are therefore captured by $\eta_t$ (the disturbance of the latent volatility process). The shock $\eta_t$ in Equation (2) can be re-written as

$$\eta_{t+1} = \rho\epsilon_t + \sqrt{1-\rho^2}\eta^*_{t+1} \tag{4}$$

with $\eta^*_{t+1} \sim N\left(0,1\right)$ and $\eta^*_{t+1} \perp \epsilon_t$. The standard SV model corresponds to $\rho = 0$. The innovation $\eta_t$ captures the total effects of uncertainty shocks after taking into account the change in the first moment of credit growth rate and the disturbance $\eta^*_t$ captures the pure (independent) effects of a change in the second moment.

## 2.3 Bayesian Estimation

For Bayesian inference, the joint posterior distribution of $\theta$ and $h_{1:T}$ is

$$p\left(\theta, h_{1:T}|y_{1:T}\right) = \frac{p\left(h_{1:T}, y_{1:T}|\theta\right)p\left(\theta\right)}{p\left(y_{1:T}\right)}; \tag{5}$$

$$p\left(h_{1:T}, y_{1:T}|\theta\right) = p\left(h_1|\theta\right) p\left(y_1|h_1, \theta\right) p\left(h_2|h_1, y_1, \theta\right) p\left(y_2|h_2, y_1, \theta\right) \prod_{t=3}^{T} p\left(h_t|h_{t-1}, y_{t-1}, y_{t-2}, \theta\right) p\left(y_t|h_t, y_{t-1}, \theta\right); \tag{6}$$

$p\left(\theta\right)$ is the prior density for $\theta$; and

$$p\left(y_{1:T}\right) = \int_{\Theta} p\left(y_{1:T}|h_{1:T}, \theta\right) p\left(h_{1:T}|\theta\right) p\left(\theta\right) dh_{1:T} d\theta, \tag{7}$$

is the marginal likelihood. The vector of model parameters for the univariate SV model with leverage is $\{\overline{\mu_h}, \phi_y, \phi_h, \tau, \rho\}$.

The likelihood function for the univariate SV model is computationally intractable because it is a high dimensional integral over the latent states $h_{1:T}$. Andrieu et al. (2010) propose the pseudo marginal Metropolis-Hastings (PMMH) method for Bayesian inference in state space models; PMMH carries out Markov chain Monte Carlo (MCMC) on an expanded space using an unbiased estimate $\widehat{p}\left(y_{1:T}|\theta, u\right)$ of the likelihood $p\left(y_{1:T}|\theta\right)$, where $u$ is the set of random numbers used to construct the likelihood estimator. Given that the PMMH is currently at $(\theta, u)$, the PMMH sampler accepts a proposal $\left(\theta^{'}, u^{'}\right)$ with the acceptance probability

$$\min\left\{1, \frac{\widehat{p}\left(y_{1:T}|\theta^{'}, u^{'}\right) p\left(\theta^{'}\right)}{\widehat{p}\left(y_{1:T}|\theta, u\right) p\left(\theta\right)} \frac{q\left(\theta|\theta^{'}\right)}{q\left(\theta^{'}|\theta\right)}\right\}. \tag{8}$$

Algorithm 1 in Appendix A outlines the standard PMMH method.

Pitt et al. (2012) show that under idealised conditions the variance of the log of the estimated likelihood should be around 1 for the optimal performance of the PMMH method, and that the performance of the method deteriorates exponentially as the variance of the log of the estimated likelihood increases beyond 1. However, a drawback of PMMH is that it is sensitive to the size of the variance of the log of the estimated likelihood, so that for many problems it is computationally demanding to ensure that variance of the log of the estimated likelihood is around 1; e.g. Fernández-Villaverde et al. (2011) use the PMMH method with 2000 particles to obtain the unbiased estimate of the likelihood. Deligiannidis et al. (2018) refined the PMMH method by correlating the pseudo random numbers $u$ and $u^{'}$ used in estimating the likelihood at the current and proposed values of the Markov chain to reduce the variance of $\log \widehat{p}\left(y_{1:T}|\theta^{'}, u^{'}\right) - \log \widehat{p}\left(y_{1:T}|\theta, u\right)$ appearing in (8). The correlated PMMH approach helps the chain to mix even if highly variable estimates of the likelihood are used; this means that generally far fewer particles are required at every iteration of the MCMC than for the standard PMMH. Algorithm 2 in Appendix B describes the correlated PMMH algorithm. The backward simulation algo-

rithm in Godsill et al. (2004) is used to sample the latent log-volatility; Algorithm 3 in the appendix C describes the correlated particle filter algorithm to obtain the unbiased estimate of the likelihood.

We follow Kim et al. (1998) and choose the prior for the persistence parameters $\phi_y$ and $\phi_h$ as $(\phi+1)/2 \sim \text{Beta}(a_0 = 20, b_0 = 1.5)$, i.e.

$$p(\phi) = \frac{1}{2B(a_0, b_0)} \left(\frac{1+\phi}{2}\right)^{a_0-1} \left(\frac{1-\phi}{2}\right)^{b_0-1}. \tag{9}$$

The prior for $\tau$ is the half-Cauchy distribution, i.e. $p(\tau) = (2I(\tau > 0))/(\pi(1+\tau^2))$ , the prior for $p(\overline{\mu_h}) \propto 1$, and the prior for $p(\rho) \sim U(-1, 1)$. These prior densities cover most possible values in practice, are non-informative, and independent.

The correlated PMMH sampler was run for 15000 iterations, with the initial 5000 iterations discarded as burn-in. We use an adaptive random walk proposal for $q(\theta'|\theta)$ and, following Garthwaite et al. (2016), adaptively tune the scaling factor of the covariance matrix. This enables us to pre-specify the overall acceptance probability before running the correlated PMMH method. In the examples, the overall acceptance probability is set as 25% and the number of particles to 100.

# 3 Empirical Results

We now discuss the results from estimating the stochastic volatility model with and without leverage effects. Table 1 reports the posterior mean estimates of the stochastic volatility parameters (with 95% credible intervals in brackets) for the growth rate in total credit available to the nonfinancial sector. The table shows that: (1) the parameter estimates of the basic SV model assuming $\rho = 0$ are similar to the parameter estimates of the SV model with leverage (allowing for correlation between shocks to the level and variance of credit-growth). Next, we consider the parameter estimates of the SV model with leverage; (2) the average volatility of an innovation to total credit, $\overline{\mu_h}$, is large revealing a large degree of volatility in the credit growth and the posterior of $\overline{\mu_h}$ is tightly concentrated; (3) there is substantial evidence for stochastic volatility in the data for credit-growth rate (a large $\tau$); (4) the shocks to the level and log-volatility of total credit are quite persistent (large $\phi_y$ and $\phi_h$); (5) the credible interval for the correlation parameter $\rho$ is wide; although, allowing for the leverage effect increases the precision with which most parameters are estimated ($\tau$, $\phi_y$, $\phi_h$). In section 6.3 we report these estimates across different measures of credit to show that time-variation in credit-uncertainty is a robust empirical feature.

Figure 2 plots the posterior mean estimate for the volatility process from the SV-

**Table 1:** Posterior Mean Estimates (with 95% credible intervals in brackets) of the standard SV Model and the SV model with leverage.

| Parameters | SV | SV-leverage |
|---|---|---|
| $\overline{\mu_h}$ | $-10.12$ $(-10.77,-9.32)$ | $-10.23$ $(-10.83,-9.61)$ |
| $\phi_h$ | 0.89 (0.64,0.99) | 0.91 (0.75,0.98) |
| $\phi_y$ | 0.83 (0.73,0.91) | 0.83 (0.75,0.91) |
| $\tau$ | 0.29 (0.09,0.66) | 0.27 (0.12,0.53) |
| $\rho$ | – | 0.50 $(-0.16,0.95)$ |

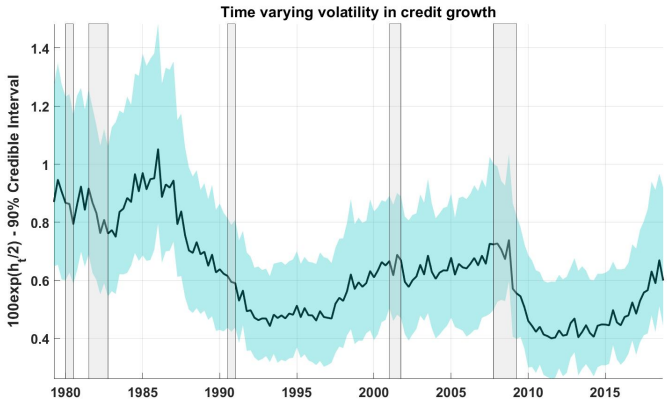


**Figure 2:** Time-varying volatility in credit growth. We plot the posterior mean estimate of the process describing the standard deviation in credit-growth: $100\exp(h_t/2)$. Shaded grey areas show NBER recessions.

leverage model[5] and its 90% credible interval; the figure shows that the second moment characterizing uncertainty in access to credit displays significant time variation. Our measure effectively distinguishes periods of high and low credit availability. The earlier part of the sample, between 1982 and 1986, is a period of high credit growth and high uncertainty in credit growth. This time period also has banking deregulation. The turning point in the late eighties shows that there is a decline in the volatility as the process of deregulation becomes fully integrated. This decline in credit volatility continues into the late 1990s when the economy witnesses a dot-com boom and bust. Figure 3 plots the estimated posterior mean for the extracted shocks along with the growth rate of credit and shows how the extracted shock moves with the business cycle process.

[5]The estimated volatility for both models – without and without leverage are comparable as implied by the estimated parameters.

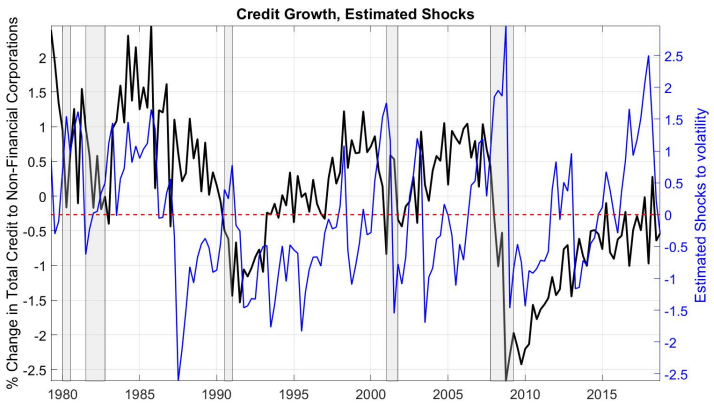


**Figure 3:** Estimated shocks to the volatility in credit growth. We plot the posterior mean estimate of the shocks that capture independent changes in uncertainty in blue, and the data on quarterly growth rate for total credit available to the nonfinancial sector in black. Shaded gray areas denote NBER recessions. We standardize the data on the growth rate of credit, and extracted shocks to capture the relative difference in the size of shocks between recessions and expansions.

To understand how the estimated latent volatility in credit growth rate relates to existing measures of uncertainty, Table 2 reports the correlation at various leads and lags for our measure of time-varying volatility and commonly used measures of uncertainty (VIX, JLN Index: Jurado, Ludvigson, and Ng (2015), BBD Index: Baker, Bloom, and Davis (2016)). While a positive correlation is observed, it is important to note that the estimate does not move one for one with these measures. The shocks are extracted from the credit market itself, so while measures such as the VIX capture aggregate uncertainty, they do not tell us whether it originates in the macro or the financial sectors of the economy; i.e., is it spiking because of a goods market shock or a financial shock. Thus

**Table 2:** Lead/Lag Correlation: Corr $(\sigma_{h,t}, Var_{x,t+k})$, where $\sigma_{h,t} = \exp(h_t/2)$ is our measure, $Var_{x,t+k}$ are the alternative measures of uncertainty defined in column 1, and $k$ is the number of quarters ahead

| Alternative measures of uncertainty | k | -3 | -2 | -1 | 0 | 1 | 2 | 3 | 4 |
|---|---|---|---|---|---|---|---|---|---|
| VIX | | 0.19 | 0.22 | 0.24 | 0.31 | 0.35 | 0.37 | 0.42 | 0.44 |
| BBD – Economic Policy Uncertainty Index | | 0.21 | 0.23 | 0.24 | 0.29 | 0.27 | 0.25 | 0.27 | 0.31 |
| JLN – Macro Uncertainty Index/h=1 | | 0.37 | 0.40 | 0.43 | 0.48 | 0.52 | 0.53 | 0.54 | 0.53 |
| JLN – Real Uncertainty Index/h=1 | | 0.29 | 0.31 | 0.34 | 0.38 | 0.40 | 0.42 | 0.42 | 0.42 |
| JLN – Financial Uncertainty Index/h=1 | | 0.10 | 0.13 | 0.18 | 0.23 | 0.27 | 0.29 | 0.32 | 0.31 |

far, the dynamics of the second moment characterizing credit-uncertainty are examined. This measure distinguishes periods of easy availability of credit from periods of a credit

crunch and low credit availability. Having established these empirical regularities, we next consider the importance of this process in generating business cycle fluctuations.

# 4 Real effects of shocks to credit-uncertainty

Do shocks to credit-uncertainty have real effects? To answer this question we use the extracted shocks to credit-uncertainty and construct local projections as in Jordà (2005). Equation (10) describes our specification for constructing the regime-independent responses of macroeconomic variables at horizon $h$ for shocks to credit-uncertainty in period $t$,

$$x_{t+h} = \alpha_h + \psi_h(L)z_{t-1} + \beta_h shock_t + \epsilon_{t+h} \ ; \tag{10}$$

$x$ is the macroeconomic variable of interest, $z$ is a vector of control variables, $\psi_h(L)$ is a second-order polynomial in the lag operator, and shock is the identified shock – either $\eta_t^*$ or $\eta_t$ from the stochastic volatility model in section 2. The baseline control variables include lags of the GDP growth rate, lags of the dependent variable, lags of a financial stress index[6], and lags of the quarterly credit growth rate. The macroeconomic variables considered for constructing local projections include credit-dependent measures of real activity (total vehicle sales and durable consumption) as well as broader measures of macroeconomic activity (aggregate consumption, non-durable consumption, investment, GDP, unemployment rate and total employed). To understand the effects on credit markets, we also examine the effect on the growth rate of household leverage and the difference between Baa and Aaa corporate bond yields.

We follow Ramey and Zubairy (2018) to account for state dependence and examine the presence of heterogeneity in the response of macroeconomic variables for shocks to credit-uncertainty in recessions and expansions, and extend the linear model in Equation (10) to

$$\begin{aligned} x_{t+h} = I_{t-1}[\alpha_{R,h} + \psi_{R,h}(L)z_{t-1} + \beta_{R,h}shock_t + \epsilon_{t+h}] \\ + (1 - I_{t-1})[\alpha_{NR,h} + \psi_{NR,h}(L)z_{t-1} + \beta_{NR,h}shock_t + \epsilon_{t+h}] \ . \end{aligned} \tag{11}$$

Equation (11) allows for state dependence in calculating impulse responses; $I_{t-1}$ is a dummy variable indicating whether the state of the economy is in a recession when the shock hits. All the model coefficients are allowed to vary according to the state of the economy. To account for the serial correlation in the error terms, the Newey-West correction is used for the standard errors.

[6]We use the Chicago Fed's National Financial Conditions Index (NFCI) to control for the state of financial conditions.

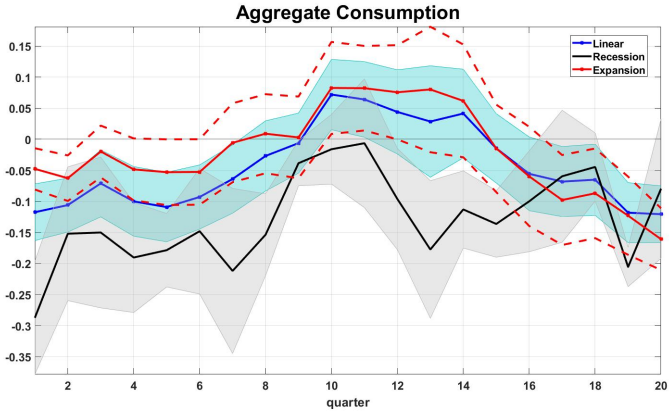


**Figure 4:** Impact of changes in $\eta_t^*$. Impulse responses calculated for the quarterly real growth rate of aggregate consumption. The blue line is the effect of a one standard deviation shock to $\eta_t^*$ in the linear model (shaded blue area – 68% CI). The black line is the effect of a one standard deviation shock to $\eta_t^*$ in recessions (shaded gray area – 68% CI). The red line is the effect of a one standard deviation shock to $\eta_t^*$ in expansions (dashed red line – 68% CI).

The results are presented in two parts. First, Figures 4, 5 and 6 isolate the effects of a pure shock to the second moment, $\eta_t^*$. Second, Figures 7 and 8 plot the total effect of a shock to uncertainty, $\eta_t$, after accounting for a change in the first moment of credit growth rate and its uncertainty. This decomposition provides a novel insight by capturing the pure effects of time-variation in uncertainty and how it interacts with changes in the first moment. The impulse responses are computed using growth rates (log-first differences) of total vehicle sales, aggregate consumption, durable consumption, non-durable consumption, investment, GDP, unemployment, non-farm employment, and household leverage. The shocks are standardized such that the coefficients in Equation (10) and (11) can be interpreted as the elasticity of the relevant variable with respect to a one-standard deviation increase in uncertainty.

## 4.1 Impact of a "pure" uncertainty shock ($\eta_t^*$)

We begin the discussion of our results by highlighting the importance of state-dependence in quantifying the effects of 'pure' shocks to credit-uncertainty. We do this by first comparing the prediction from the linear model with the prediction from the model allowing state-dependence. For analyzing the differences in the predictions from the linear model vis-à-vis the state-dependent model, we focus on the response of aggregate consumption in Figure 4. Figures 5 and 6 focus on the differential effects of shocks to credit-uncertainty in recessions and expansions across all the variables.

Impulse responses from the linear model shows that an increase in credit-uncertainty

(after removing the effects of a shock to the first moment) is contractionary. However, once we decompose the effects across recessions and expansions, we find that the real effects of credit-uncertainty are mainly observed in downturns. In recessions while we observe amplified effects, the effect of changes in uncertainty about credit access in expansions is negligible across the broad set of variables considered in the analysis. To take a deeper look at this asymmetry we revisit the expressions for calculating linear and state-dependent impulse responses in Eqs. 12 and 13 respectively.

$$x_{t+h} = \alpha_h + \psi_h(L)z_{t-1} + \beta_h shock_t + \epsilon_{t+h} \; ; \tag{12}$$

$$x_{t+h} = I_{t-1}[\alpha_{R,h} + \psi_{R,h}(L)z_{t-1} + \beta_{R,h} shock_t + \epsilon_{t+h}] + (1 - I_{t-1})[\alpha_{NR,h} + \psi_{NR,h}(L)z_{t-1} + \beta_{NR,h} shock_t + \epsilon_{t+h}]; \tag{13}$$

On comparing the Equations 12 and 13, we can see that the linear model captures the average response across recessions and expansions. In the absence of a state-dependent examination of impulse responses, the asymmetry in the effects of shocks to credit-uncertainty would be lost. Figure 4 shows that for the linear model, a shock to credit-uncertainty is contractionary and on impact aggregate consumption decreases by 0.1%. On decomposing the effects across recessions (black line) and expansions (red line) we see that the effects of credit-uncertainty matter largely during downturns where the decline in consumption is three times larger in comparison to the linear model and six times larger in comparison to expansions. In Section D of the appendix we plot the impulse responses for all the macroeconomic variables, comparing the prediction from the linear model along with the responses for recessions and expansions to show that the linear model consistently underestimates the impact of credit-uncertainty across all the variables considered in the analysis.

Qualitatively, the results from the linear model align with the empirical regularities characterizing the effects of aggregate uncertainty using alternative measures such as the VIX (Bloom, 2009), the JLN index (Jurado et al., 2015). The bigger effect in recessions is similar to those in Chatterjee (2018) and reinforce the importance of state-dependence in examining the effects of uncertainty shocks.

Having illustrated this difference between the linear and state-dependent impulse responses, in Figures 5 and 6 we focus on the asymmetric impact of shocks to credit-uncertainty in recessions and expansions.[7] During downturns, macroeconomic variables,

[7]In Sections E and F of the appendix, we show impulse responses of macroeconomic variables for a pure uncertainty shock where the shock has been constructed using data on the growth rate in consumer credit and nonfinancial business debt instead of total credit available to the nonfinancial sector as the underlying measure for credit growth. Irrespective of variable choice in estimating the uncertainty shock, the asymmetry of transmission in recessions and expansions across a broad measure of macro economic activity is consistently observed.

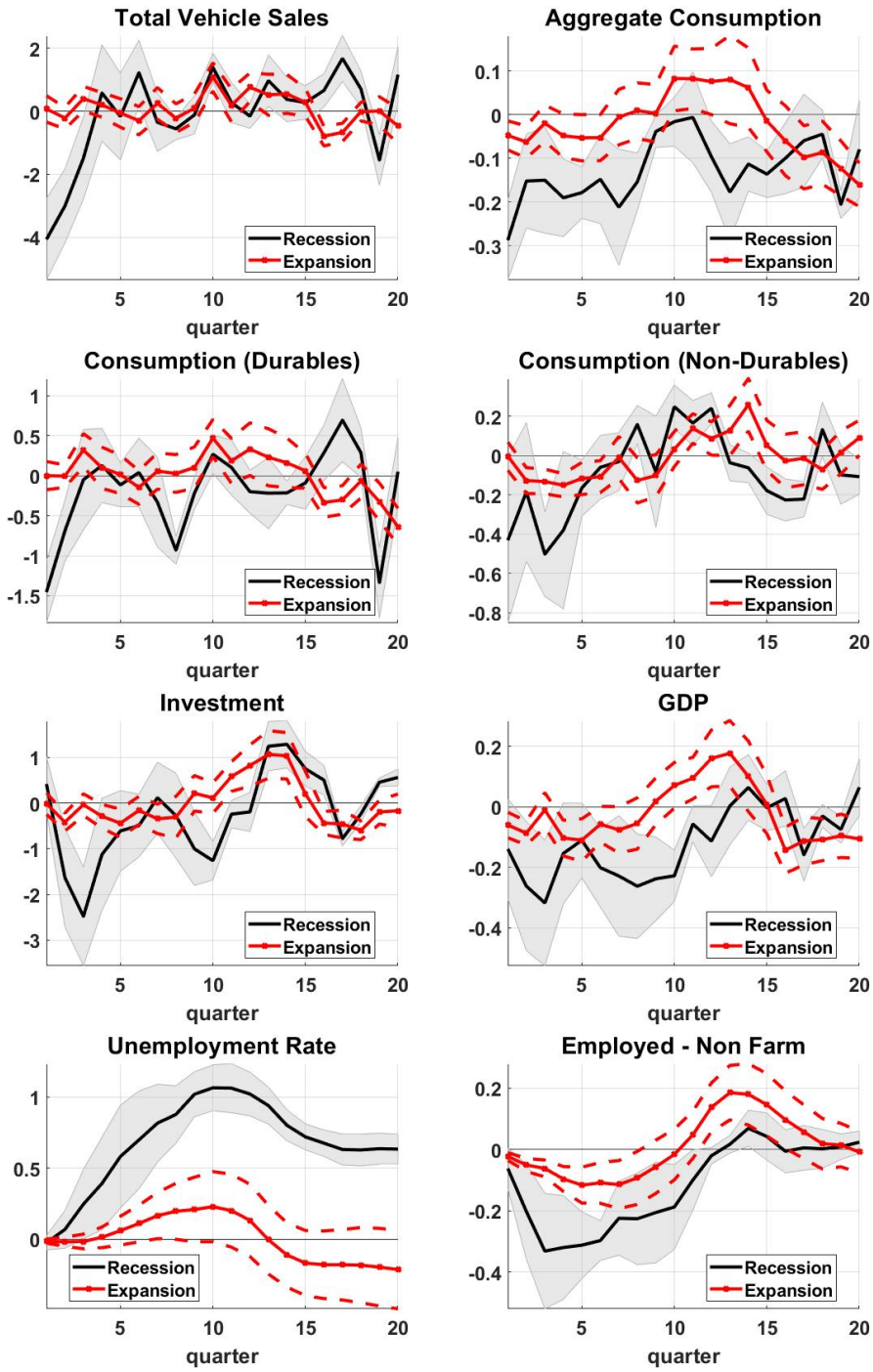


**Figure 5:** Impact of changes in $\eta_t^*$ on real activity. Impulse responses calculated for the quarterly real growth rate of total vehicle sales, durable consumption, total consumption, non-durable consumption, investment, GDP, the unemployment rate and total employed in the non-farm sector. The black line is the effect of a one standard deviation shock to $\eta_t^*$ in recessions (shaded gray area – 68% CI). The red line is the effect of a one standard deviation shock to $\eta_t^*$ in expansions (dashed red line – 68% CI).

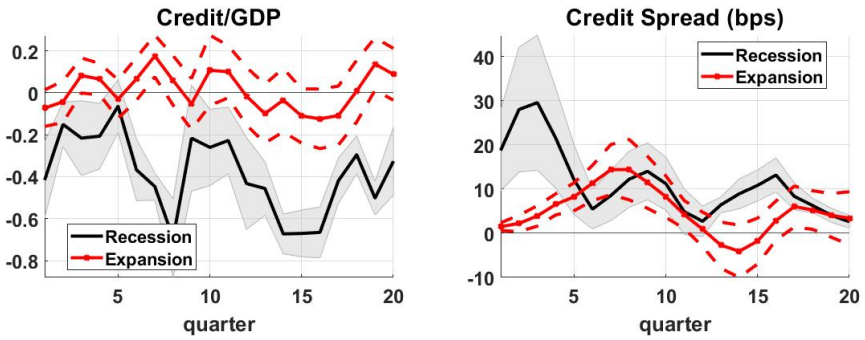


**Figure 6:** Impact of changes in $\eta_t^*$ on credit markets. Impulse responses calculated for the growth rate of household leverage (household credit/GDP) and the difference between Baa and Aaa corporate bond yields. The black line is the effect of a one standard deviation shock to $\eta_t^*$ in recessions (shaded gray area – 68% CI). The red line is the effect of a one standard deviation shock to $\eta_t^*$ in expansions (dashed red line – 68% CI).

such as vehicle sales and durable consumption, that are relatively more credit-dependent, show a sharper decline compared to broader measures of activity such as aggregate consumption. Conversely, non-durable consumption shows a significant slowdown in the periods following a shock. Investment, like the credit-sensitive components of consumption, also records a sharper slowdown. The unemployment rate peaks ten quarters after the initial shock in response.[8] In addition to examining the response of the unemployment rate we also examine the response of total employed and find that there is significant decline on impact as well as persistent effects in the quarters following the shock. When the effects across these measures of activity are combined, we find that GDP declines as well.[9]

To understand the effects on household debt and corporate borrowing costs, Figure 6 examines the impulse responses of household leverage and the difference between the 3-month Baa and Aaa corporate bond yields. The conclusions are similar to those for the macroeconomic variables – the effects are bigger during downturns. The extent of asymmetry in response is particularly prominent for the Baa-Aaa spread – the peak response is a 30 basis point increase in recessions occurring within 5 quarters of the shock as opposed to a peak response of about 15 basis points in expansions occurring 8 quarters after the shock.

The dynamics of credit spreads in recessions have been studied in different forms; the

[8]The amplified response of the unemployment rate in recessions is qualitatively similar to what has been shown in Caggiano, Castelnuovo, and Groshenny (2014) who examine the impact of uncertainty shocks on unemployment dynamics in recessions, however using the VIX as a proxy for uncertainty. Our results using shocks to credit-uncertainty suggest quantitatively bigger effects.

[9]We plot the response of net-exports and the trade-weighted real exchange rate as well for the U.S. in Section G of the appendix.

work of Christiano et al. (2015), for instance, captures the movement of the credit spread through the financial wedge by incorporating a tax on the gross rate of return on capital; in our set-up we are able to quantify the source of shock that stems directly from the movement in credit aggregates and in turn generates a spike in the Baa-Aaa spread on impact during downturns.

Figures 5 and 6 thus establish the asymmetric effects of shocks to credit-uncertainty for macroeconomic variables in recessions and expansions. An additional takeaway from this analysis is understanding the causes of a slow recovery following a recession. Jordà et al. (2013) find that recovery following a financial recession is slower in comparison to a recovery following a non-financial recession. Our results suggest the changes in the second moment capturing credit-uncertainty can exacerbate both the depth and duration of a recession and, hence, lead to a slower recovery.

## 4.2 Impact of an uncertainty shock with level effects ($\eta_t$)

So far, we examined impulse responses to changes in uncertainty after removing the effects of shocks to the first moment. This analysis is important as it emphasizes the importance of 'pure' shocks to the second moment describing credit-uncertainty.

Figure 3 shows that shocks to uncertainty spike during recessions when there is also a sharp decline in the growth rate of credit (in expansions, uncertainty about credit access can co-move positively with credit growth, especially in the mid 1980s). We now focus on shocks to credit-uncertainty that embeds changes in the first-moment characterizing credit-growth. To understand the effects of uncertainty that reflect changes in the first-moment, we look at the impulse responses of macro variables for $\eta_t$.[10] Figures 7 and 8 examine the effects the shocks to uncertainty after accounting for the change in the first moment.

We report the impulse responses for the recessionary regime only as our results suggest that the impact in expansions is negligible. The solid black line in each figure captures the effects of shocks to uncertainty after removing the effects of the first moment and is identical to the results reported for the recessionary regime in Figures 4, 5 and 6. The solid blue line in each figure captures the effects after allowing for interaction between the first and second moment.

These results are important, as they allow us to quantify the effects of aggregate uncertainty by considering the interaction with the first moment. While existing studies examine the time-variation of uncertainty in periods of elevated financial stress, they do not quantify the real effects by taking into account the interaction between shocks to the

[10]The expression for the uncertainty shock embedding first moment implications is given by: $\eta_t = \rho\epsilon_{t-1} + \sqrt{1-\rho^2}\eta_t^*$. $\eta_t^*$ is the pure/independent component.

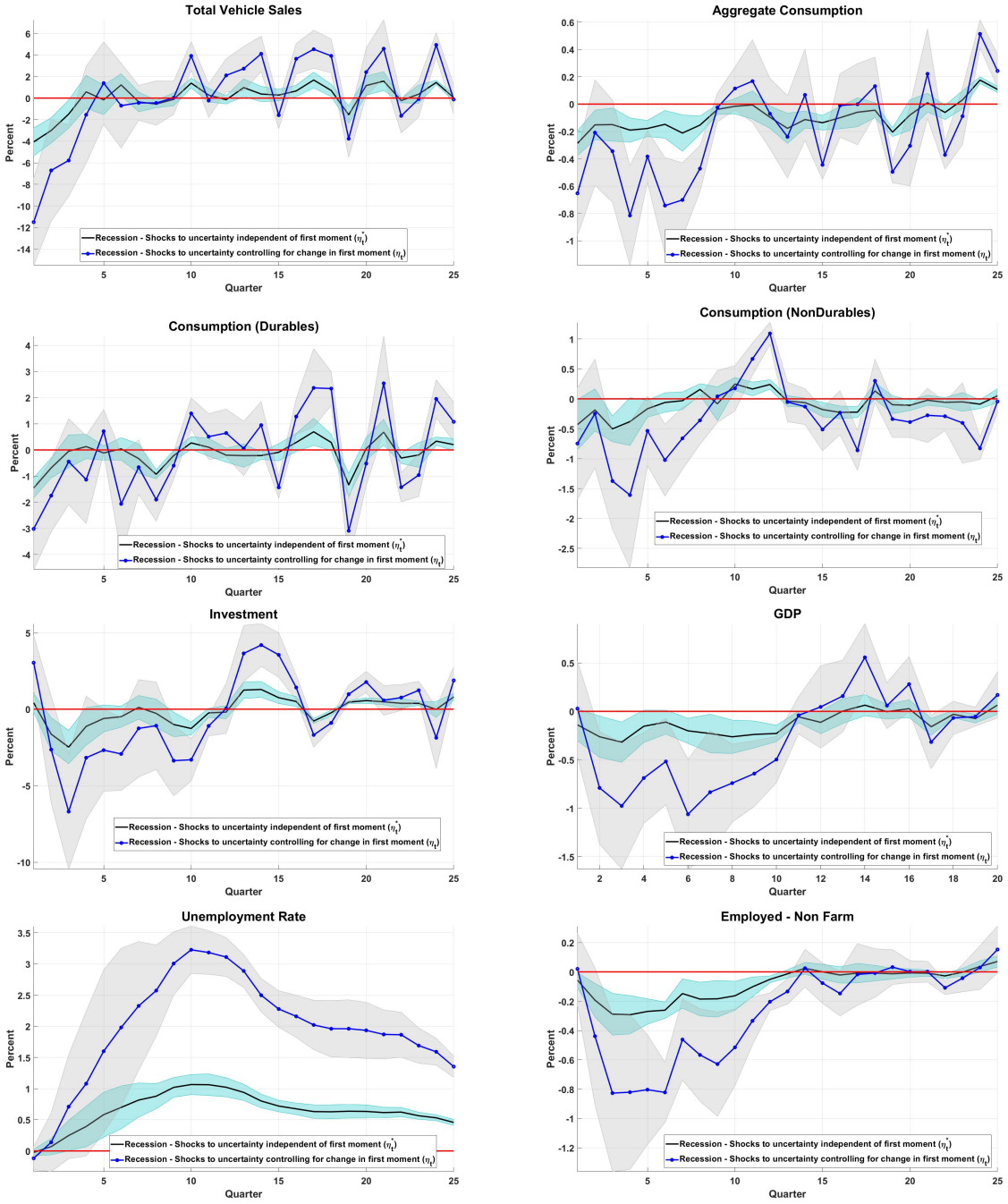


**Figure 7:** Impact of changes in $\eta_t$ on real activity. Impulse responses calculated for the quarterly real growth rate of total vehicle sales, durable consumption, total consumption, non-durable consumption, investment, GDP, the unemployment rate and total employed in the non-farm sector. The blue line is the effect of a one standard deviation shock to $\eta_t$ in recessions (shaded gray area – 68% CI). The black line is the effect of a one standard deviation shock to $\eta_t^*$ in recessions (shaded blue area – 68% CI).

first and second moments.

The decline in the credit-sensitive components of consumption, after taking into ac-

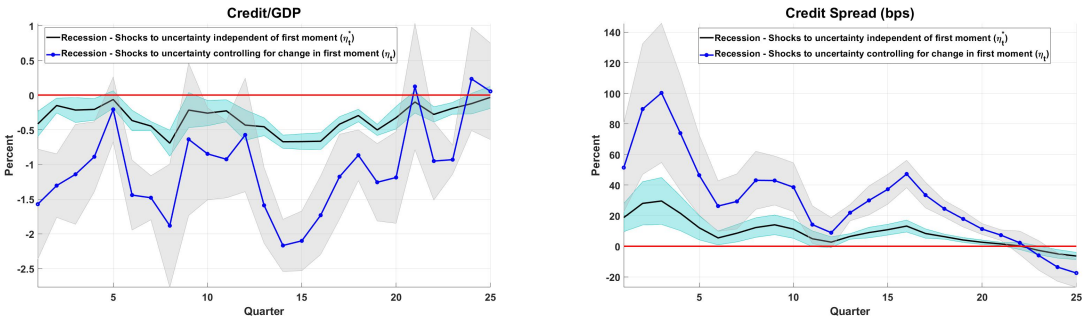


**Figure 8:** Impact of changes in $\eta_t$ on credit markets. Impulse responses calculated for the growth rate of household leverage (household credit/GDP) and the difference between Baa and Aaa corporate bond yields. The blue line is the effect of a one standard deviation shock to $\eta_t$ in recessions (shaded gray area – 68% CI). The black line is the effect of a one standard deviation shock to $\eta_t^*$ in recessions (shaded blue area – 68% CI).

count the decline in the credit growth rate and increase in credit-uncertainty, is about three times higher for both the growth rate of vehicle sales and durable consumption, compared to the impact of a pure shock to uncertainty. As before, a significant impact is observed two periods after the shock for non-durable consumption. Across all variables, there is an amplification in the slowdown once the second moment shock is allowed to interact with shocks to the first moment.

Thus far, we have examined the empirical importance of our extracted shocks. In the next section, we develop a theoretical model to provide intuition and understand the channels of transmission for our proposed shock.

# 5 Theoretical Model

We use a model of collateral constraints in the spirit of Kiyotaki and Moore (1997) as a theoretical framework for interpreting the empirical results. In a simple real business cycle (RBC) model, a role for credit frictions is introduced by incorporating a working capital requirement on the firms' side. We assume that at the beginning of each period, firms must pay labor prior to production of output. Firms finance this labor payment with an intratemporal loan.[11] There is no interest rate on financing the working capital because the firms pay off the loans within the period. However, the amount that a firm can borrow is limited to a fraction of the value of firm capital. The specification of the model environment follows Sims (2017). The novelty of our model lies in introducing uncertainty through a stochastic volatility channel in credit availability that directly

[11] We abstract from intertemporal debt in the baseline model. The intuition governing the impact of an uncertainty shock remains unchanged compared to the scenario with intertemporal debt.

interacts with the ability of the firm to borrow.

## 5.1 Model Description

This is a model in discrete time where agents live infinitely. Households consume ($C_t$), supply labor ($N_t$) and save ($B_t$); $R_t$ is the gross rate of return on savings. Household utility is of CRRA type, additively separable in labor and consumption; $\gamma_c$ is inverse of the intertemporal elasticity of substitution, $\chi$ is the inverse of the Frisch elasticity, $\beta$ is the discount factor, and $\theta$ is set such that in steady state, the hours supplied is one-third. Households optimize:

$$\max_{\{C_t, N_t, B_{t+1}\}} E_0 \sum_{t=0}^{\infty} \beta^t \left( \frac{C_t^{1-\gamma_c}}{1-\gamma_c} - \theta \frac{N_t^{1+\chi}}{1+\chi} \right)$$

subject to

$$C_t + B_{t+1} = W_t N_t + R_{t-1} B_t + \Pi_t \ ;$$

$W_t$ is the real wage and $\Pi_t$ denotes residual profits from firms. The first order conditions of the household are

$$C_t^{-\gamma_c} = \lambda_t \ ; \tag{14}$$

$$\theta N_t^{\chi} = \lambda_t W_t \ ; \tag{15}$$

$$1 = \beta E_t \Big[ \Big( \frac{C_{t+1}}{C_t} \Big)^{-\gamma_c} R_t \Big] \ . \tag{16}$$

The firms own capital stock ($K_t$) and hire labor input ($N_t$) from households to produce output $Y_t$ using the Cobb-Douglas production technology

$$Y_t = A_t K_t^{\alpha} N_t^{1-\alpha} \ ; \tag{17}$$

$A_t$ describes the state of aggregate technology. Capital accumulation is subject to adjustment costs and evolves as

$$K_{t+1} = (1-\delta) K_t + I_t - \frac{\phi}{2} \Big( \frac{I_t}{K_t} - \delta \Big)^2 K_t \ ; \tag{18}$$

$I_t$ is investment, $\delta$ is the rate at which capital depreciates and $\phi$ is the cost of adjusting capital. In this framework, investment is financed using residual profits (dividends). The dividend payout is

$$\Pi_t = Y_t - w_t N_t - I_t \ .$$

We introduce a working capital constraint in this simple RBC setup and assume that firms must pay labor prior to producing output and the working capital is financed through an

intratemporal loan. The constraint restricting working-capital financing is

$$W_t N_t \leq \zeta_t q_t K_t \tag{19}$$

The amount the firm can borrow as seen from Eq. 19, is limited to a fraction $\zeta_t$ of the total value of capital, with $q_t$ the price of capital. $q_t$ is the shadow price of capital and is defined using the Lagrange multiplier on the law of motion of capital in the optimization problem of the firm that we discuss below. The firm chooses investment ($I_t$), capital ($K_{t+1}$) and labor ($N_t$) by maximizing the the discounted sum of dividends ($\Pi_t$)

$$\max_{\{I_t, N_t, K_{t+1}\}} E_0 \sum_{t=0}^{\infty} \beta^t \frac{\lambda_t}{\lambda_0} \Big[ A_t K_t^{\alpha} {N_t}^{1-\alpha} - W_t N_t - I_t \Big]$$

subject to the law of motion for capital (Eq. 18) and the constraint restricting working-capital financing (Eq. 19). Firm dividends at time $t+j$ are discounted using the stochastic discount factor from the optimization problem of the households – $\beta^j \lambda_{t+j}/\lambda_t$. Let $\mu_t$ be the multiplier on the working capital constraint; $\mu_t > 0$ implies that the constraint binds and changes in $\zeta_t$ impact the equilibrium conditions of the model. The first order conditions corresponding to the optimal choices of investment ($I_t$), labor ($N_t$) and capital ($K_{t+1}$) are

$$W_t(1+\mu_t) = (1-\alpha) A_t K_t^{\alpha} N_t^{-\alpha} \ , \tag{20}$$

$$1 = q_t \Big[ 1 - \phi\Big( \frac{I_t}{K_t} - \delta \Big) \Big] \ , \tag{21}$$

$$q_t = \beta E_t \frac{\lambda_{t+1}}{\lambda_t} \left[ \alpha A_{t+1} K_{t+1}^{\alpha-1} N_{t+1}^{1-\alpha} + q_{t+1} \left( (1-\delta) + \mu_{t+1}\zeta_{t+1} - \frac{\phi}{2}\Big( \frac{I_{t+1}}{K_{t+1}} - \delta \Big)^2 + \phi\Big( \frac{I_{t+1}}{K_{t+1}} - \delta \Big) \frac{I_{t+1}}{K_{t+1}} \right) \right] \ , \tag{22}$$

and

$$\mu_t (W_t N_t - \zeta_t q_t K_t) = 0 \text{ with } \mu_t \geq 0 \ . \tag{23}$$

When the credit constraint binds, $\mu_t > 0$ and $(W_t N_t - \zeta_t q_t K_t) = 0$; when the constraint is slack, $\mu_t = 0$ and $(W_t N_t - \zeta_t q_t K_t) < 0$. The market clearing condition is

$$Y_t = C_t + I_t \ . \tag{24}$$

We assume that the fraction of the value of the firm that can be borrowed follows an AR(1) process with a time-varying second moment,

$$\begin{aligned} \zeta_t - \zeta_{ss} &= \rho(\zeta_{t-1} - \zeta_{ss}) + \exp(h_t/2)\epsilon_t \ , \\ h_t &= (1-\rho_h)\overline{h} + \rho_h h_{t-1} + \tau \eta_t^* \ ; \end{aligned} \tag{25}$$

$\zeta_{ss}$ is the fraction the firm can borrow against the value of capital in steady state; $\overline{h}$ is the average uncertainty in credit availability; and $\tau$ is the extent of stochastic volatility in credit availability. The specification of stochastic volatility in the model is identical to what is estimated in Section 2 and is similar to what has been presented in Fernández-Villaverde et al. (2011), Fernández-Villaverde et al. (2015), and Fernández-Villaverde and Guerrón-Quintana (forthcoming).[12] Ceteris paribus, a shock to the first moment of $\zeta_t$ ($\epsilon_t$) in the model relaxes the borrowing constraint and firms have access to more credit. Likewise, a shock to the second moment of $\zeta_t$ ($\eta_t^*$) generates uncertainty about credit available in the economy. We introduce a collateral constraint in a flexible price DSGE model and interpret the relaxation and tightening of credit availability vis-à-vis shocks to $\zeta_t$. This simple set-up captures the essence of the transmission of shocks to volatility about credit availability. The first moment implications of credit access are frequently studied (for e.g.: Jermann and Quadrini (2012)); however, our findings show that this second moment describing credit-uncertainty by itself can generate important implications for real activity and business cycles. Equations (14)-(25) summarize the equilibrium conditions in the model.

## 5.2 Model Calibration

The model is calibrated quarterly and the behavioral parameters of the model are standard. The share of capital in the Cobb-Douglas production function is set at $\alpha = 0.33$, the discount factor $\beta = 0.99$, the rate of depreciation of capital $\delta = 0.02$, and investment adjustment costs $\phi = 4$. The parameter $\theta$ scaling the disutility of labor supply is set to 5.7063 so that labor hours in steady state are $\frac{1}{3}$. The inverse interemporal elasticity of substitution is fixed at $\gamma_c = 1$ and the inverse of the Frisch elasticity of labor supply at $\chi = 1$. We set the state of aggregate technology $A_t$ to 1.

We next calibrate the steady-state value of $\zeta_t$ and the parameters governing the evolution of $\zeta_t$. Note that when the collateral constraint binds in steady state, $\mu > 0$, it imposes certain restrictions on the steady state values of $\zeta_t = \zeta_{ss}$. For $\mu > 0$ in steady state, it can be shown that $\zeta_{ss} < \frac{1-\alpha}{\alpha}\left(\frac{1}{\beta} - (1-\delta)\right)$. Given the values of $\alpha, \beta, \delta$, we find that $\zeta_{ss} < 0.0602$. To match the uncertainty in the model with what we find in the data, we revisit the posterior estimates presented in Table 1 of section 3 and calibrate the parameters guiding the evolution of $\zeta_t$ using the estimates describing credit-uncertainty in the data. We think this approach captures the impact of unforeseen changes of credit availability (first order as well as second order) in the data as well as the model; with positive (negative) shocks to $\zeta_t$ implying higher (lower) availability of credit in the data

[12] Our results are robust to the alternative specification in Basu and Bundick (2017).

as well as relaxing (tightening) of the borrowing constraint in the representative agent model. The same intuition works for a shock to the second moment as well.

We set $\overline{h} = \overline{\mu_h} = -10.12$, $\rho_h = \phi_h = 0.91$, $\tau = 0.25$ and $\rho = \phi_y = 0.83$, corresponding to the posterior means obtained from the estimates in section 3. The steady-state value of $\zeta_t = \zeta_{ss}$ is calibrated to 1.75%. This calibration implies that the standard deviation of shocks to the first moment of $\zeta_t$ is $\exp(\overline{\mu_h}/2) = 0.0063$.[13] The specification of the stochastic volatility process is exactly the same as in the model presented in section 2. We set the correlation coefficient between shocks to the first moment and second moment to zero so that we can focus on the effects of shocks to credit-uncertainty by itself.

## 5.3 Model Solution

The goal of this paper is to explore the effects of a change in the second moment that captures uncertainty shocks to credit constraints. A first order approximation shuts down the effects of changes in higher-order moments by construction. A second-order solution impacts expected values but does not influence the dynamics as higher-order terms do not independently enter the solution (Schmitt-Grohé and Uribe, 2004). It is necessary to consider a third-order approximation for uncertainty to have dynamic effects. We do so by using the perturbation methods combined with pruning (to prevent explosive solutions) in Andreasen, Fernández-Villaverde, and Rubio-Ramírez (2018). The credit constraint always binds.

## 5.4 Transmission of shock to uncertainty

The behavior of the firm in this environment is subject to collateral constraints on borrowing. Since the constraint limits the quantity a firm may borrow, it has implications for how much labor the firm can hire. That is, it introduces a wedge between the frictionless competitive equilibrium and the realized outcome in the constrained economy. This simple assumption generates important implications by introducing a distortion between labor demanded by firms and labor supplied by households.

Basu and Bundick (2017) show that in a flexible-price model, an uncertainty shock introduced through time variation in the volatility of household preferences cannot generate a simultaneous decline in consumption, investment, and output; this is regarded as a stylized fact that characterizes the effect of an uncertainty shock. Basu and Bundick

[13] We could alternately calibrate the evolution of $\zeta_t$ using parameters describing stochastic volatility in nonfinancial business debt. The parameters are similar to what we find from estimation using data on total credit extended to the private nonfinancial sector and presented in section 6.3. The results remain unchanged with this alternative calibration. We also carry out robustness checks to different values of $\zeta_{ss}$ in section 6.2.

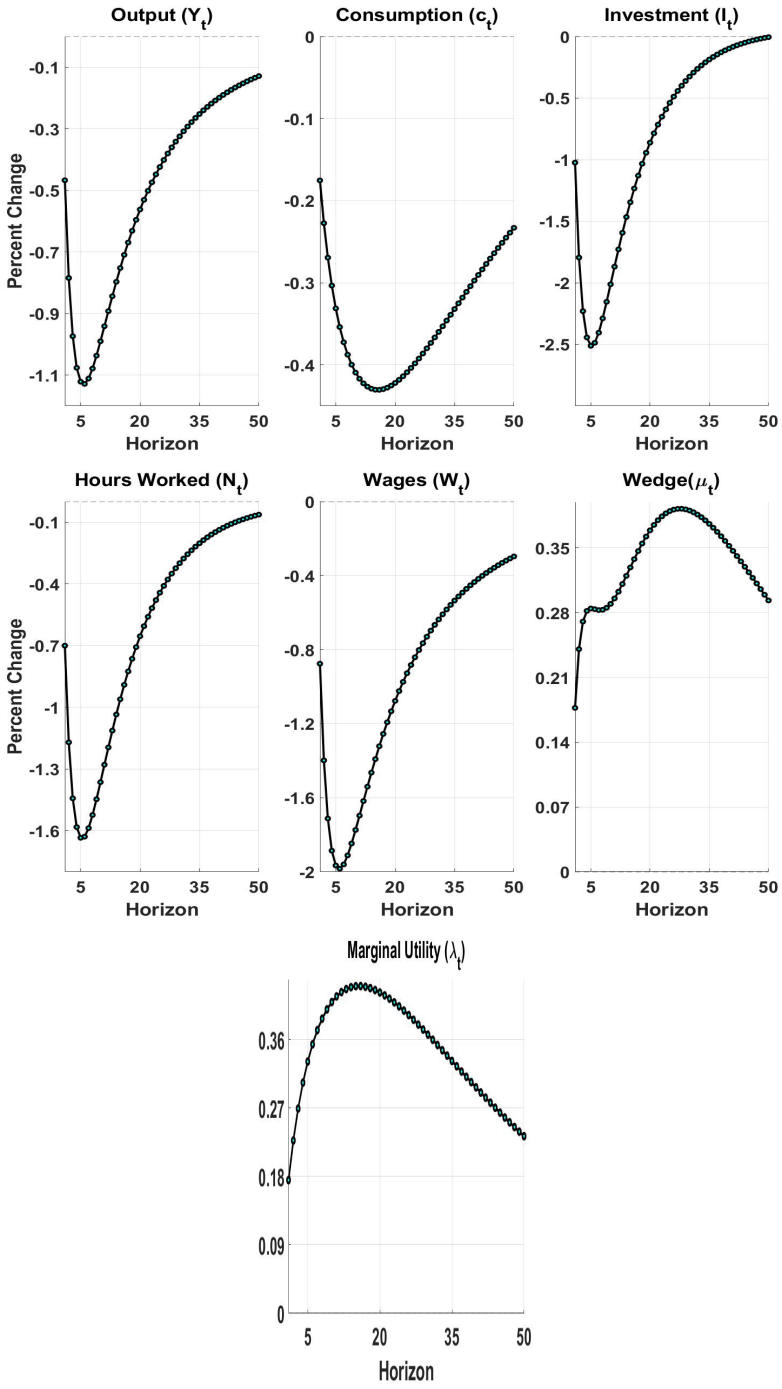


**Figure 9:** Impulse responses for a 1 standard deviation shock to uncertainty $\eta_t^*$ in the DSGE model. A shock to credit uncertainty triggers a simultaneous decline in output, consumption, investment, hours, and real wages.

(2017) subsequently highlight the importance of nominal rigidities through the wedge introduced by the presence of a mark-up in labor demand. In our environment, however we introduce uncertainty through a credit channel. The collateral constraint in our model,

operating through the intratemporal working capital channel, distorts the flexible price equilibrium. The labor demand side of the model now reflects the effect of the collateral constraint

$$W_t(1+\mu_t) = (1-\alpha)A_t K_t^{\alpha} N_t^{-\alpha} \ ;$$

the labor supply side remains unaffected by this distortion;

$$W_t = \frac{\theta N_t^{\chi}}{C_t^{-\gamma_c}}.$$

An uncertainty shock in the model triggers a precautionary saving response by households, leading to decrease in consumption, an increase in marginal utility and an increase in labor supply. In a flexible price model, this increase in labor supply is absorbed and thus prevents the simultaneous decline in consumption, investment and output. In a flexible price model with collateral constraints, when there is an uncertainty shock to $\zeta_t$ that limits that amount that a firm can borrow, the multiplier on the borrowing constraint now provides the additional margin that is provided by the mark-up in a model with sticky prices. When there is an exogenous shock to credit-uncertainty – here interpreted as a shock to the second moment of $\zeta_t$ – there is an increase in $\mu_t$, the Lagrange multiplier on the binding constraint, which prevents labor demand from increasing and in turn generates sizable and simultaneous declines in hours, real wages, output, consumption and investment.

To better understand how the precautionary motives interact with the endogenous variables, we now examine the expression for the third-order accurate solution of the model and focus exclusively on third-order effects.[14] Following Andreasen et al. (2018), the expression that *only* preserves the third-order effects for the control variables after pruning is,

$$y_t^{3rd} = g_v \begin{bmatrix} x_{t-1}^{3rd} \\ 0 \\ 0 \end{bmatrix} + 2G_{vv}\left( \begin{bmatrix} x_{t-1}^{f} \\ \epsilon_t \\ \eta_t^* \end{bmatrix} \otimes \begin{bmatrix} x_{t-1}^{s} \\ 0 \\ 0 \end{bmatrix} \right) + G_{vvv}\left( \begin{bmatrix} x_{t-1}^{f} \\ \epsilon_t \\ \eta_t^* \end{bmatrix} \otimes \begin{bmatrix} x_{t-1}^{f} \\ \epsilon_t \\ \eta_t^* \end{bmatrix} \otimes \begin{bmatrix} x_{t-1}^{f} \\ \epsilon_t \\ \eta_t^* \end{bmatrix} \right) + \frac{3}{6} g_{\sigma\sigma v}\sigma^2 \begin{bmatrix} x_{t-1}^{f} \\ \epsilon_t \\ \eta_t^* \end{bmatrix} + \frac{1}{6} g_{\sigma\sigma\sigma}\sigma^2$$

The vector of state variables, is $x_t = [K_t, \zeta_t, h_t, \sigma]$ for our model, and the vector of

[14] Schmitt-Grohé and Uribe (2004) show that up to a second-order, independent changes in uncertainty shocks do not impact the dynamics. The dynamic effects of uncertainty can be obtained as third-order effects from a third-order approximation.

shocks is $[\epsilon_t, \eta_t^*]$. $K_t$ is the level of capital stock, $\zeta_t$ is the fraction of value of capital against which the firm can borrow, $h_t$ is the time-varying variance of $\zeta_t$, and $\sigma$ is the perturbation parameter. $\epsilon_t$ is a shock to the first moment of $\zeta_t$ and $\eta_t^*$ is a shock to the second moment of $\zeta_t$. Here, $x_t^f$ preserves the first-order effects, $x_t^s$ preserves the second-order effects, and, $x_t^{rd}$ preserves the third-order effects for the state variables in the DSGE model. The extended state space vector for higher-order solution includes the second and third-order terms along with the usual first-order effects.[15] The matrix $g_v$ summarize the coefficients at the first-order. The matrices $G_{vv}$ and $G_{vvv}$ summarize the coefficients corresponding to the interaction terms at the second and third-order, respectively; $g_{\sigma\sigma\nu}$ captures the direct effect of an uncertainty shock for a third-order approximation; and since all innovations in our model have symmetric distributions $g_{\sigma\sigma\sigma}$ is a vector with all elements equal to 0.[16]

A change in $\eta_t^*$ captures an uncertainty shock in the model. Using the third-order solution, we decompose the impulse response on impact for a shock to credit-uncertainty into two parts; a direct effect and an interaction effect. On impact, an uncertainty shock has a direct effect on the endogenous variables through $\eta_t^*$, and the size of the impact is obtained by the relevant coefficients of the matrix $g_{\sigma\sigma v}$ for the control variables.[17] Column 1 of Table 3 reports direct effects.

We now isolate the interaction effects. Under a rational expectations assumption, agents can observe the shock to uncertainty about credit access $\eta_t^*$ at time $t$, hence,

[15] The extended state space vector is given as follows: $\Big[x_{t-1}^f, x_{t-1}^s, x_{t-1}^{3^{rd}}, \epsilon_t, \eta_t^*, x_{t-1}^f \otimes x_{t-1}^f, x_{t-1}^f \otimes \epsilon_t, x_{t-1}^f \otimes \eta_t^*, \epsilon_t \otimes \epsilon_t, \epsilon_t \otimes \eta_t^*, \eta_t^* \otimes \eta_t^*, x_{t-1}^f \otimes x_{t-1}^s, x_{t-1}^f \otimes x_{t-1}^f \otimes x_{t-1}^f, x_{t-1}^f \otimes x_{t-1}^f \otimes \epsilon_t, x_{t-1}^f \otimes x_{t-1}^f \otimes \eta_t^*, x_{t-1}^f \otimes \epsilon_t \otimes \epsilon_t, x_{t-1}^f \otimes \epsilon_t \otimes \eta_t^*, x_{t-1}^f \otimes \eta_t^* \otimes \eta_t^*, \epsilon_t \otimes \epsilon_t \otimes \epsilon_t, \epsilon_t \otimes \epsilon_t \otimes \eta_t^*, \epsilon_t \otimes \eta_t^* \otimes \eta_t^*, \eta_t^* \otimes \eta_t^* \otimes \eta_t^*\Big]$. $\otimes$ is the Kronecker product.

[16] The effect on the state variables that only preserves the third-order effects after pruning is similarly obtained, from,

$$x_t^{3rd} = h_v \begin{bmatrix} x_{t-1}^{3rd} \\ 0 \\ 0 \end{bmatrix} + 2H_{vv}\left( \begin{bmatrix} x_{t-1}^f \\ \epsilon_t \\ \eta_t^* \end{bmatrix} \otimes \begin{bmatrix} x_{t-1}^s \\ 0 \\ 0 \end{bmatrix} \right) + H_{vvv}\left( \begin{bmatrix} x_{t-1}^f \\ \epsilon_t \\ \eta_t^* \end{bmatrix} \otimes \begin{bmatrix} x_{t-1}^f \\ \epsilon_t \\ \eta_t^* \end{bmatrix} \otimes \begin{bmatrix} x_{t-1}^f \\ \epsilon_t \\ \eta_t^* \end{bmatrix} \right) + \frac{3}{6} h_{\sigma\sigma v}\sigma^2 \begin{bmatrix} x_{t-1}^f \\ \epsilon_t \\ \eta_t^* \end{bmatrix} + \frac{1}{6} h_{\sigma\sigma\sigma}\sigma^2$$

The matrix $h_v$ summarize the coefficients at the first-order. The matrices $H_{vv}$ and $H_{vvv}$ summarize the coefficients corresponding to the interaction terms at the second and third-order, respectively; $h_{\sigma\sigma\nu}$ captures the direct effect of an uncertainty shock for a third-order approximation; and since all innovations in our model have symmetric distributions $h_{\sigma\sigma\sigma}$ is a vector with all elements equal to 0. For a detailed exposition on the pruned third-order solution, refer to equations (65) and (66) in the Appendix to Andreasen et al. (2018).

[17] In our model $\dim(g_{\sigma\sigma v}) = 5 \times 5$. So the fifth column of this matrix captures the non-zero effects of an uncertainty shock.

**Table 3:** Decomposing the effects of an uncertainty ($\eta_t^*$) shock on impact

| Variables | Direct Effect of $\eta_t^*$ (% change) (1) | Interaction Effect of $\eta_t^* E_t(\epsilon_t, \epsilon_t)$ (% change) (2) | Total Effect (% change) (3) |
|---|---|---|---|
| Consumption | -0.097 | -0.078 | -0.175 |
| Real Wages | -0.04 | -0.836 | -0.876 |
| Rate of Return on Capital | -0.084 | 0.008 | -0.076 |
| GDP | 0.039 | -0.505 | -0.466 |
| Hours | 0.058 | -0.758 | -0.7 |
| Marginal Utility | 0.097 | 0.078 | 0.175 |
| Wedge | 0.046 | 0.132 | 0.178 |
| Price of Capital | 0.018 | -0.06 | -0.042 |
| Investment | 0.226 | -1.251 | -1.025 |

$E_t\eta_t^* = \eta_t^*$. If the impulse responses are computed at the nonstochastic steady state, then on impact all $(t-1)$ dated variables are 0, that is, $x_{t-1}^f = 0, x_{t-1}^s = 0, x_{t-1}^{rd} = 0$; therefore, $E_t(x_{t-1}^f x_{t-1}^s) = 0$. Additionally, the interaction terms of the form $E_t(x_{t-1}^f \epsilon_t \eta_t^*)$, $E_t(x_{t-1}^f \epsilon_t \epsilon_t)$, $E_t(x_{t-1}^f \eta_t^* \eta_t^*)$, and $E_t(x_{t-1}^f \eta_t^* \epsilon_t)$ can be expressed as $\eta_t^* E_t(x_{t-1}^f \epsilon_t)$, $E_t(x_{t-1}^f \epsilon_t \epsilon_t)$, $\eta_t^{*2} E_t(x_{t-1}^f)$, and $\eta_t^* E_t(x_{t-1}^f \epsilon_t)$; these terms are zero since the shocks to the first moment are uncorrelated with $x_{t-1}^f$; the remaining interaction terms are $E_t(\epsilon_t \epsilon_t \epsilon_t)$, $E_t(\epsilon_t \epsilon_t \eta_t^*)$, $E_t(\epsilon_t \eta_t^* \eta_t^*)$ and $E_t(\eta_t^* \eta_t^* \eta_t^*)$.

A shock to $\eta_t^*$ implies that the effects on the interaction terms are $\eta_t^* E_t(\epsilon_t \epsilon_t)$, $\eta_t^{*2} E_t(\epsilon_t)$ and $\eta_t^{*3}$. Given that $\epsilon_t \underset{iid}{\sim} (0,1)$, $\eta_t^* \underset{iid}{\sim} (0,1)$, $E_t(\eta_t^* \epsilon_t) = 0$, $E_t \epsilon_t = 0$, and $E_t(\epsilon_t \epsilon_t) = 1$, the non-zero interaction effect in the extended state space shows up for $\eta_t^* E_t(\epsilon_t \epsilon_t)$. For a model with symmetric shocks, the coefficients corresponding to $\eta_t^{*3}$ are 0. The interaction effects for a shock to $\eta_t^*$ are therefore captured by the coefficients corresponding to $\eta_t^* E_t(\epsilon_t \epsilon_t)$ in the $G_{vvv}$ matrix. Column 2 of Table 3 reports the effect on impact attributed to the interaction channel. Column 3 of Table 3 summarizes the total effect on impact = the sum of the direct effect and interaction effect. An advantage of this decomposition is that it helps isolate the precautionary savings driven change in hours supplied and the contraction in hours demanded that works through the wedge $\mu_t$.

Column 1 of Table 3 shows that the direct effect of an uncertainty shock clearly generates a precautionary decline in consumption, an increase in the marginal utility, hours, and investment.[18] However, there is also an increase in the wedge $\mu_t$ through the direct effect. Column 2 of Table 3 shows that the interaction effects between these

[18]Given that capital is a state variable, investment has to increase in response to the direct effect if there a decline in consumption and increase in labor supply since this is a closed economy model and $Y_t = C_t + I_t$.

different elements dampens total hours supplied, GDP and investment, but amplifies the initial decline in consumption from the precautionary response. Column 3 of Table 3 presents total effects, and correspond to the response on impact in Figure 9 discussed above. In a sticky price environment, the excess labor supply (row 5 of Column 1 in Table 3) cannot be absorbed as the markup responds endogenously to precautionary driven increase in labor supply; however with the presence of the wedge now entering through the collateral constraint, there is an inward shift of the labor demand curve that is captured by the response of hours (row 5 Column 2 in Table 3).

If the decline in labor is sufficiently strong, the decline in output is accompanied by a sharp fall in investment along with a decline in consumption. This decomposed view of interpreting the impact of uncertainty explicitly quantifies the different channels through which the shock is transmitted in our model.

These results operate through the firm's binding borrowing constraint and are insightful as an uncertainty shock of this form generates a simultaneous decline in hours, real wages, consumption, investment, and output in a parsimoniously specified environment. One of the challenges in the theoretical literature examining the effects of uncertainty has been to generate a sizable and simultaneous impact for endogenous variables in response to changes in the second moment. Our proposed shock and model with a collateral constraint can generate a significant impact on macroeconomic variables in response to changes in uncertainty. The model predictions thus match the patterns recovered from empirically analyzing the effects of shocks to credit-uncertainty in Section 4.1, as well as building intuition about the cause of the slowdown in activity.

# 6 Extensions and Robustness

Thus far, we have been examining the propagation of a shock to credit-uncertainty to the real economy. The impulse responses in section 5.4 show that an increase credit-uncertainty is recessionary and the transmission relies on an interaction between the borrowing constraint faced by firms and the precautionary saving response from the households. The baseline model can provide an empirically-consistent explanation for the response of aggregate variables. In this section we consider a simple extension of the model presented in section 5, evaluate the robustness of results to calibrated parameters in the model; we also check the robustness of our empirical results to using different measures of credit-growth, different choice of prior and different sample size.

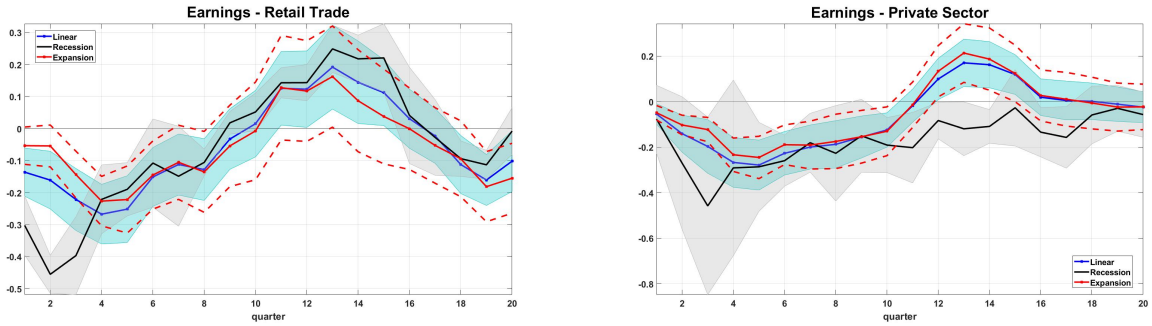


**Figure 10:** Impact of changes in $\eta_t^*$ (pure shock to uncertainty) on earnings for retail trade and private sector as a whole. Impulse responses calculated for the quarterly real growth rate of income calculated using hours and hourly earnings for retail trade and the private sector as a whole. The blue line is the effect of a one standard deviation shock to $\eta_t^*$ in the linear model (shaded blue area – 68% CI). The black line is the effect of a one standard deviation shock to $\eta_t^*$ in recessions (shaded gray area – 68% CI). The red line is the effect of a one standard deviation shock to $\eta_t^*$ in expansions (dashed red line – 68% CI).

## 6.1 Extension with hand-to-mouth consumers

We consider a simple extension of the framework examined in section 5.1 and introduce heterogeneity in the description of households. The motivation to consider this extension is twofold. First, the transmission of shock to credit-uncertainty relies on the interaction between the precautionary savings motive by the households and the wedge stemming from the borrowing constraint faced by firms. The idea is to understand the importance of the collateral constraint when the precautionary channel is diluted. Second, we examine the empirical impulse responses of quarterly earnings for the retail trade sector and the private sector as a whole.[19] Figure 10 shows that on impact earnings for those working in retail trade decline significantly on impact, whereas, the decline for the private sector as a whole can be seen several quarters after the shock. The population capturing those employed in retail trade can be interpreted as agents with limited access to savings and consumption smoothing.

In the theoretical environment we capture these features by incorporating hand-to-mouth consumers. Within the continuum of infinitely lived households we introduce a fraction $\nu$ that do not have access to savings, and therefore do not own any assets or liabilities and in each period consume their labor income. These are the hand-to-mouth consumers or the non-Ricardian households. The remaining $(1-\nu)$ fraction of households are able to save as before. The non-Ricardian households are important as they cannot

[19] We construct the empirical measure of quarterly earnings using data on average hourly earnings and weekly hours and then examine the growth rate to remove the effects of time trend. Impulse responses have been constructed using the method of local projections and the estimated shock on credit-uncertainty as in section 4.

engage in precautionary savings behavior. Along with the responses of GDP, investment, and aggregate consumption, we examine the consumption response of the non-Ricardian households to understand if they are more vulnerable to the effects of uncertainty in the economy.

The equilibrium conditions of the model are now updated to reflect this feature of heterogeneity. The behavior of the Ricardian households is identical to those in the baseline model in Section 5.1. The hand-to-mouth/non-Ricardian agents maximize period utility

$$\max_{\{C_t^{NR}, N_t^{NR}\}} \left( \frac{C_t^{NR\,1-\gamma_c}}{1-\gamma_c} - \theta_R \frac{N_t^{NR\,1+\chi}}{1+\chi} \right)$$

subject to

$$C_t^{NR} = W_t N_t^{NR} \ .$$

The first order conditions give

$$N_t^{NR} = \left( \frac{W_t^{1-\gamma_c}}{\theta_R} \right)^{\frac{1}{\chi+\gamma_c}} \ . \tag{26}$$

The parameter $\theta_R$ is chosen such that hours supplied by the non-Ricardian agents in steady state is 1/3. In addition to Eq. 26, aggregate consumption and hours now reflect the heterogeneity in households,

$$C_t = \nu C_t^{NR} + (1-\nu) C_t^R \tag{27}$$

and

$$N_t = \nu N_t^{NR} + (1-\nu) N_t^R \ . \tag{28}$$

Before we proceed to examining the impulse responses, we would like to highlight some features of the model setup. The labor supply for the hand-to-mouth agents is fixed when $\gamma_c = 1$. The implications for earning and consumption for the hand-to-mouth consumers, therefore, stem completely from the dynamics of labor demand, and the contraction in labor demand is brought about by the interaction between the wedge ($\mu_t$) and the uncertainty shock. The value of $\nu$ is now set to 11.5.%[20] The baseline model presented in sections 5.1 through 5.4 corresponds to $\nu = 0$. In the data, earnings are measured by a product of hours worked and hourly earnings. In the theoretical environment, consumption by the hand-to-mouth consumers also equals the product of wages and hours. We use this relation to compare the responses of aggregate consumption and the consumption of the hand-to-mouth agents. Figure 11 compares the prediction from the

[20]This captures the ratio of total employed in retail trade to total employed in the non-farm sector.

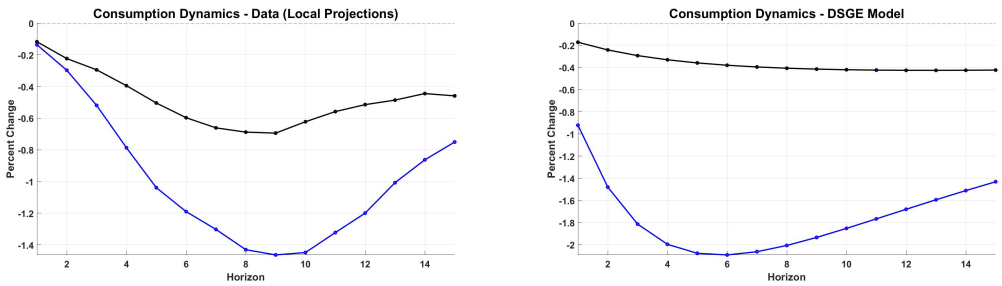


**Figure 11:** Comparing the response of aggregate consumption and consumption/earnings of hand-to-mouth/non optimizing agents.

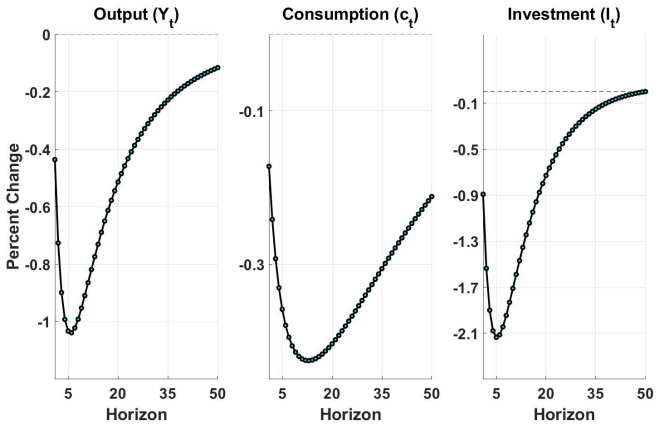


**Figure 12:** Impulse responses of output, aggregate consumption and investment with hand-to-mouth agents.

model with what we find in the data and shows that introducing heterogeneity in savings behavior can generate the amplified decline for the hand-to-mouth consumers. Moreover, as shown in Figure 12, even with the precautionary channel diluted, the increase in the wedge stemming from the borrowing constraint on firms is recessionary and can generate a decline in key macroeconomic variables.

## 6.2 Differential effects

In the empirical analysis we highlight the asymmetry in the effects of shocks to credit-uncertainty in recessions and expansions. In the theoretical environment, we do not distinguish between recessions and expansions. One way to potentially address the differential effects across recessions and expansions in the theoretical model is by changing the steady state value of the collateral constraint. The intuition guiding this choice is as follows. When $\zeta_{ss}$ is closer to the limiting value of 0.0602, the constraint is closer to

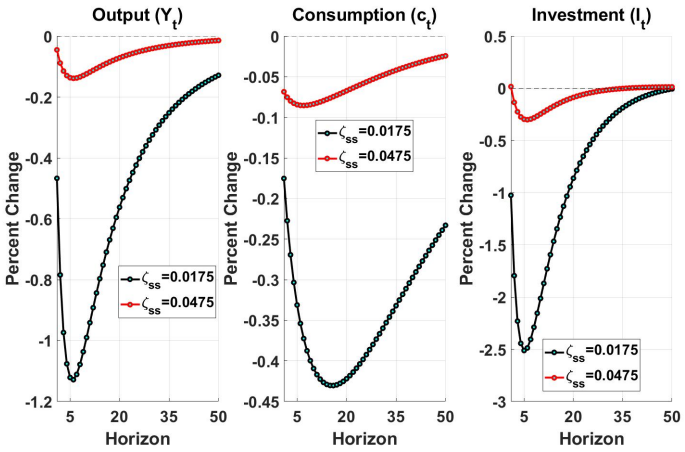


**Figure 13:** Impulse responses of output, aggregate consumption and investment for different values of $\zeta_t$ in steady state. In a recession the collateral constraint is farther from slackness ($\zeta_{ss} = 0.0175$) compared to expansions ($\zeta_{ss} = 0.0475$).

being slack as opposed to when the steady state value is farther away and closer to zero.[21] We present impulse responses for different values of $\zeta_{ss}$ in Figure 13 that can indirectly capture the effects of recessions and expansions; with expansions being captured by the calibration of $\zeta_t$ that is closer to slackness (0.0475).[22] Note that despite different values of $\zeta_{ss}$ the simultaneity in the decline of output, consumption and investment is preserved.

## 6.3 Robustness Checks

This section carries out some robustness checks of the empirical results by considering alternative choice of priors for the SV parameters, taking a longer sample for the series $\{y_t\}$, and considering other measures of credit. Table 4 summarizes the results.

**Alternative choice of prior:** We use the following tighter priors for the SV model $p(\phi_y) = p(\phi_h) \sim TN_{(0,1)}(0.9, 0.05^2)$, $p(\overline{\mu_h}) \sim N(0, 10^2)$, $p(\tau) \sim TN_{(0,\infty)}(0.5, 0.3^2)$, and $p(\rho) \sim U(-1, 1)$. The $TN_{(lo,up)}(c, d^2)$ denotes the univariate normal distribution with mean $c$ and standard deviation $d$ constrained to the interval $(lo, up)$. We denote the results with alternative prior as $y_t^P$ in Table 4. The estimation in section 2 uses uninformative priors.

**Longer sample:** In section 2, we estimate the model using data between 1979 Q1 to 2018 Q4. We estimate the model using an extended sample between 1952Q1-2018Q4.

[21] While calibrating the model parameters we show that the parameters in the model imply that in steady state $\zeta_t < 0.0602$.

[22] Guerrieri and Iacoviello (2017) in their analysis find that the collateral constraint on housing wealth becomes slack during expansions and tightens during the Great Recession.

**Table 4:** Posterior Mean Estimates (with 95% credible intervals in brackets)

| Parameters | $y_t$ – Baseline | $y_t^P$ | $y_t^L$ | $x_t$ | $c_t$ | $z_t$ |
|---|---|---|---|---|---|---|
| $\overline{\mu_h}$ | −10.23 (−10.83,−9.61) | −10.22 (−10.85,−9.67) | −9.80 (−10.90,−9.06) | −10.06 (−10.8,−9.55) | −8.06 (−8.53,−7.65) | −10.14 (−10.5,−9.80) |
| $\phi_h$ | 0.91 (0.75,0.98) | 0.91 (0.83,0.97) | 0.97 (0.93,0.99) | 0.86 (0.61,0.99) | 0.78 (0.49,0.99) | 0.89 (0.78,0.96) |
| $\phi_y$ | 0.83 (0.75,0.91) | 0.84 (0.78,0.91) | 0.73 (0.62,0.83) | 0.82 (0.72,0.93) | 0.22 (0.09,0.37) | 0.81 (0.73,0.88) |
| $\tau$ | 0.27 (0.12,0.53) | 0.29 (0.15,0.55) | 0.16 (0.08,0.28) | 0.32 (0.09,0.63) | 0.38 (0.05,0.78) | 0.30 (0.17,0.47) |
| $\rho$ | 0.50 (−0.16,0.95) | 0.45 (−0.21,0.92) | 0.42 (−0.06,0.76) | −0.32 (−0.76,0.2) | 0.55 (0.09,0.82) | 0.77 (0.42,0.95) |

We denote the results for the extended sample as $y_t^L$ in Table 4.

**Alternative definitions of credit:** Sections 2-5 examine the presence and impact of shocks to the second moment using *Total Credit to Private nonfinancial Sector* as a measure of credit growth. This is a broad measure and captures credit extended to non-financial corporations, households and non-profit institutions serving households. To understand if our results are robust to alternative definitions of credit, we carry out the estimation using data on credit extended to nonfinancial businesses (debt securities and loans; liability) – ($x_t$ in Table 4),[23] consumer credit owned by households ($c_t$ in Table 4)[24] along with an alternative measure of total credit available in the macroeconomy – debt securities, loans and liability in all sectors ($z_t$ in Table 4).[25]

Table 4 shows that the parameter estimates of the SV model are very similar between the three scenarios suggesting that the results are robust against prior specification and different lengths of the datasets. For alternative definitions of credit as well, we find that this evidence stochastic volatility is a common and robust feature.

# 7 Conclusion

In this paper, we present a new stylized fact that characterizes the time variation in the volatility of credit growth. We interpret this stochastic volatility in credit growth as credit-uncertainty. Our results suggest that unforeseen changes in credit-uncertainty can trigger a sharp slowdown in real activity. We empirically distinguish between the effects in expansions and recessions and show that these effects are asymmetric in nature – and

[23]The series has been taken from the Financial Accounts of the United States. For details on composition see `https://www.federalreserve.gov/apps/fof/SeriesAnalyzer.aspx?s=LA144104005&t=`

[24]The series has been taken from the Financial Accounts of the United States. For details on composition see `https://www.federalreserve.gov/apps/fof/SeriesAnalyzer.aspx?s=FL153166000&t=L.101&suf=Q`

[25]The series has been taken from the Financial Accounts of the United States. For details on composition see `https://www.federalreserve.gov/apps/fof/SeriesAnalyzer.aspx?s=FL894104005&t=`

matter during downturns. Shocks to credit-uncertainty have a significant impact on real activity during busts; while during booms the effects are negligible and uncertainty about credit access does not impede the pace of real activity. We exploit the dynamics of credit expansion and contraction to extract uncertainty shocks and introduce a channel that potentially explains the slowdown in the pace of recovery following a crash.

To provide intuition for the transmission mechanism, we present a flexible-price model with collateral constraints and examine the effects of a shock to credit-uncertainty in this framework. We find that when the collateral constraint binds, unforeseen changes in credit-uncertainty transmits by triggering a precautionary response that interacts with the collateral constraint to generate a sizable and simultaneous decline in output, consumption, investment, real wages, and hours. This interaction is a novel feature and generates the simultaneous decline in these variables that previous work on uncertainty shocks without credit constraints has been unable to produce in a flexible price environment.

# References


Piergiorgio Alessandri and Haroon Mumtaz. Financial regimes and uncertainty shocks. *Journal of Monetary Economics*, 101:31–46, 2019.

Ivan Alfaro, Nicholas Bloom, and Xiaoji Lin. The finance uncertainty multiplier. *Working Paper*, 2019. URL `https://nbloom.people.stanford.edu/research`.

Martin M. Andreasen, Jesús Fernández-Villaverde, and Juan F Rubio-Ramírez. The pruned state-space system for non-linear DSGE models: Theory and empirical applications. *Review of Economic Studies*, page 1–49, 2018.

C. Andrieu, A. Doucet, and R. Holenstein. Particle Markov chain Monte Carlo. *Journal of Royal Statistical Society Series B*, pages 1–33, 2010.

Cristina Arellano, Yan Bai, and Patrick J. Kehoe. Financial frictions and fluctuations in volatility. *Journal of Political Economy*, 127(5):2049–2102, 2019.

Scott R. Baker, Nicholas Bloom, and Steven J. Davis. Measuring economic policy uncertainty. *The Quarterly Journal of Economics*, 131(4):1593–1636, 2016.

Susanto Basu and Brent Bundick. Uncertainty shocks in a model of effective demand. *Econometrica*, pages 937 –958, 2017.

David Berger, Ian Dew-Becker, and Stefano Giglio. Uncertainty shocks as second-moment news shocks. *The Review of Economic Studies*, 87(1):40–76, 2020.

Nicholas Bloom. The impact of uncertainty shocks. *Econometrica*, page 623–685, 2009.

Nicholas Bloom, Max Floetotto, Nir Jaimovich, Itay Saporta-Eksten, and Stephen J Terry. Really uncertain business cycles. *Econometrica*, pages 1031–1065, 2018.

Giovanni Caggiano, Efrem Castelnuovo, and Nicolas Groshenny. Uncertainty shocks and unemployment dynamics in U.S. recessions. *Journal of Monetary Economics*, page 78–92, 2014.

Giovanni Caggiano, Efrem Castelnuovo, S. Delrio, and R. Kima. Financial uncertainty and real activity: The good, the bad, and the ugly. *CAMA Working Paper*, 67, 2020. URL `https://ssrn.com/abstract=3192234`.

Dario Caldara, Cristina Fuentes-Albero, Simon Gilchrist, and Egon Zakrajšek. The macroeconomic impact of financial and uncertainty shocks. *European Economic Review*, 88:185 – 207, 2016.

Pratiti Chatterjee. Asymmetric impact of uncertainty in recessions: are emerging countries more vulnerable? *Studies in Nonlinear Dynamics & Econometrics*, 2018.

Lawrence J. Christiano, Roberto Motto, and Massimo Rostagno. Risk shocks. *American Economic Review*, page 27–65, 2014.

Lawrence J. Christiano, Martin Eichenbaum, and Mathias Trabandt. Nominal rigidities and the dynamic effects of a shock to monetary policy. *American Economic Journal: Macroeconomics*, pages 110–67, 2015.

G. Deligiannidis, A. Doucet, and M. K. Pitt. The correlated pseudo marginal method. *Journal of Royal Statistical Society Series B*, pages 839–870, 2018.

Jesús Fernández-Villaverde and Pablo Guerrón-Quintana. Uncertainty shocks and business cycle research. *Review of Economic Dynamics*, forthcoming.

Jesús Fernández-Villaverde, Pablo Guerrón-Quintana, Juan F Rubio-Ramírez, and Martin Uribe. Risk matters: The real effects of volatility shocks. *American Economic Review*, pages 2530–2561, 2011.

Jesús Fernández-Villaverde, Pablo Guerrón-Quintana, Keith Kuester, and Juan F Rubio-Ramírez. Fiscal volatility shocks and economic activity. *American Economic Review*, pages 3352–84, 2015.

P. H. Garthwaite, Y. Fan, and S. A. Sisson. Adaptive optimal scaling of Metropolis Hastings algorithms using the Robbins-Monro process. *Communications in Statistics - Theory and Methods*, pages 5098–5111, 2016.

Mark Gertler and Simon Gilchrist. What happened: Financial factors in the great recession. *Journal of Economic Perspectives*, 32(3):3–30, 2018.

S. Godsill, A. Doucet, and M. West. Monte Carlo smoothing for nonlinear time series. *Journal of American Statistical Association*, pages 156–168, 2004.

Luca Guerrieri and Matteo Iacoviello. Collateral constraints and macroeconomic asymmetries. *Journal of Monetary Economics*, 90:28–49, 2017.

Urban Jermann and Vincenzo Quadrini. Macroeconomic effects of financial shocks. *American Economic Review*, 102(1):238–271, 2012.

Òscar Jordà. Estimation and inference of impulse responses by local projections. *American Economic Review*, page 161–182, 2005.

Òscar Jordà, Mortiz Schularick, and Alan M. Taylor. When credit bites back. *Journal of Money, Credit and Banking*, 2013.

Kyle Jurado, Sydney C Ludvigson, and Serena Ng. Measuring uncertainty. *American Economic Review*, page 1177–1216, 2015.

S. Kim, N. Shephard, and S. Chib. Stochastic volatility: Likelihood inference and comparison with ARCH models. *The Review of Economic Studies*, pages 361–393, 1998.

Nobuhiro Kiyotaki and John Moore. Credit cycles. *Journal of Political Economy*, pages 211–248, 1997.

Sylvain Leduc and Zheng Liu. Uncertainty shocks are aggregate demand shocks. *Journal of Monetary Economics*, page 20–35, 2016.

Sydney C. Ludvigson, Sai Ma, and Serena Ng. Uncertainty and business cycles: Exogenous impulse or endogenous response? *American Economic Journal: Macroeconomics*, forthcoming.

Atif Mian and Amir Sufi. Finance and business cycles: The credit- driven household demand channel. *Journal of Economic Perspectives*, page 31–58, 2018.

M. K. Pitt, R. S. Silva, P. Giordani, and R. Kohn. On some properties of Markov chain Monte Carlo simulation methods based on the particle filter. *Journal of Econometrics*, pages 134–151, 2012.

Valerie A. Ramey and Sarah Zubairy. Government spending multipliers in good times and in bad: Evidence from us historical data. *Journal of Political Economy*, pages 850–901, 2018.

Stephanie Schmitt-Grohé and Martin Uribe. Solving dynamic general equilibrium models using a second-order approximation to the policy function. *Journal of Economic Dynamics & Control*, page 755 – 775, 2004.

Eric Sims. The basics of financial constraints. *Mimeo*, 2017.

# Appendix

## A The standard PMMH algorithm

**Algorithm 1** The pseudo marginal Metropolis-Hastings

- Set the initial values of $\theta^{(0)}$ arbitrarily.
- Sample $u \sim N(0, I)$, and run a particle filter to compute an estimate $\widehat{p}(y_{1:T}|\theta, u)$ of the likelihood and to sample the initial $h_{1:T}^{(0)}$.
- For each of the MCMC iterations, $i = 1, ..., M$,
  - Sample $\theta'$ from the proposal density $q\left(\theta'|\theta\right)$ and $u' \sim N(0, I)$
  - Run a particle filter to compute an estimate of likelihood $\widehat{p}\left(y_{1:T}|\theta', u'\right)$ and sample $h_{1:T}^{'}$.
  - With probability

$$\min\left\{1, \frac{\widehat{p}\left(y_{1:T}|\theta', u'\right) p\left(\theta'\right)}{\widehat{p}\left(y_{1:T}|\theta, u\right) p\left(\theta\right)} \frac{q\left(\theta|\theta'\right)}{q\left(\theta'|\theta\right)}\right\}; \tag{29}$$

    set $h_{1:T}^{(i)} = h_{1:T}^{'}$, $\widehat{p}(y_{1:T}|\theta, u)^{(i)} = \widehat{p}\left(y_{1:T}|\theta', u'\right)$, and $\theta^{(i)} = \theta'$; otherwise, set $h_{1:T}^{(i)} = h_{1:T}^{(i-1)}$, $\widehat{p}(y_{1:T}|\theta, u)^{(i)} = \widehat{p}(y_{1:T}|\theta, u)^{(i-1)}$, and $\theta^{(i)} = \theta^{(i-1)}$.

# B The correlated PMMH algorithm

**Algorithm 2** The correlated pseudo marginal Metropolis-Hastings (PMMH)

- Set the initial values of $\theta^{(0)}$ arbitrarily.
- Sample $u \sim N(0, I)$, and run a particle filter to compute an estimate of likelihood $\widehat{p}(y_{1:T}|\theta, u)$ and to sample the initial $h_{1:T}^{(0)}$.
- For each of the MCMC iterations, $i = 1, ..., M$,
  - Sample $\theta^{'}$ from the proposal density $q\left(\theta^{'}|\theta\right)$.
  - Sample $u^* \sim N(0, I)$, and set $u^{'} = \gamma u + \sqrt{1-\gamma^2}u^*$; $\gamma$ is the correlation between $u$ and $u^{'}$ and is set close to 1.
  - Run a particle filter to compute an estimate of likelihood $\widehat{p}\left(y_{1:T}|\theta^{'}, u^{'}\right)$ and sample $h_{1:T}^{'}$.
  - With probability in Equation (29) set $h_{1:T}^{(i)} = h_{1:T}^{'}$, $\widehat{p}(y_{1:T}|\theta, u)^{(i)} = \widehat{p}\left(y_{1:T}|\theta^{'}, u^{'}\right)$, $u^{(i)} = u^{'}$, and $\theta^{(i)} = \theta^{'}$; otherwise, set $h_{1:T}^{(i)} = h_{1:T}^{(i-1)}$, $\widehat{p}(y_{1:T}|\theta, u)^{(i)} = \widehat{p}(y_{1:T}|\theta, u)^{(i-1)}$, $u^{(i)} = u^{(i-1)}$, and $\theta^{(i)} = \theta^{(i-1)}$.

# C The Correlated Particle Filter Algorithm

This section discusses the correlated particle filter of Deligiannidis et al. (2018). We use this particle filter algorithm to sequentially approximate the joint filtering densities $\{p(h_t|y_{1:t}, \theta) : t = 1, ..., T\}$ using $N$ particles, i.e., weighted samples $\left\{h_t^{1:N}, \overline{w}_t^{1:N}\right\}$, drawn from some proposal densities $m_1(h_1)$ and $m_t(h_t|h_{t-1})$ for $t \geq 2$; see Andrieu et al. (2010) for detailed assumptions about the proposal densities. Let

$$w_1^i = \frac{p(y_1|h_1)\, p(h_1)}{m_1(h_1)}, w_2^i = \frac{p(y_2|h_2, y_1)\, p(h_2|h_1, y_1)}{m_2(h_2|h_1)}, w_t^i = \frac{p(y_t|h_t, y_{t-1})\, p(h_t|h_{t-1}, y_{t-1}, y_{t-2})}{m_t(h_t|h_{t-1})}, \tag{30}$$

for $t \geq 3$ , and $\overline{w}_t^i = \frac{w_t^i}{\sum_{j=1}^N w_t^j}$. Let $u$ be the pseudo-random vector used to obtain the unbiased estimate of the likelihood; $u$ has two components $u_{h,1:T}^{1:N}$ and $u_{A,1:T-1}^{1:N}$.

Let $u_{h,t}^i$ be the vector random variable used to generate the particles $h_t^i$ given $\theta$ and $h_{t-1}^{a_{t-1}^i}$. We write,

$$h_1^i = H\left(u_{h,1}^i; \theta\right) \text{ and } h_t^i = H\left(u_{h,t}^i; \theta, h_{t-1}^{a_{t-1}^i}\right) \text{ for } t \geq 1, \tag{31}$$

where $a_{t-1}^i$ is the ancestor index of $h_t^i$. Denote the distribution of $u_{h,t}^i$ as $\psi_{ht}(\cdot)$.

For $t \geq 2$, let $u_{A,t-1}$ be the vector of random variables used to generate the ancestor indices $a_{t-1}^{1:N}$ using the resampling scheme $\mathcal{M}\left(a_{t-1}^{1:N}|\overline{w}_{t-1}^{1:N}, h_{t-1}^{1:N}\right)$ and define $\psi_{A,t-1}(\cdot)$ as the distribution of $u_{A,t-1}$. Common choices for $\psi_{ht}(\cdot)$ and $\psi_{A,t-1}(\cdot)$ are iid $U(0,1)$ or iid $N(0,1)$ random variables. The particle filter provides the unbiased estimate of the likelihood

$$\widehat{p}(y|\theta, u) = \prod_{t=1}^{T}\left(\frac{1}{N}\sum_{i=1}^{N} w_t^i\right). \tag{32}$$

For the correlated PMMH to work efficiently, it is necessary that the logs of the likelihood estimates $\widehat{p}(y|\theta,u)$ and $\widehat{p}\left(y|\theta^{'},u^{'}\right)$ are highly correlated. The resampling steps in the particle filter introduce discontinuities even when $\theta$ and $\theta^{'}$ are only slightly different, where $\theta$ is the current value and $\theta^{'}$ is the proposed value of the parameters. The discontinuity problem is solved by first sorting the particles from the smallest to largest before resampling them. Algorithm 3 gives the correlated particle filter algorithm. At time $t=1$, step 1 generates

$$h_1^i = \sqrt{\tau^2/(1-\phi^2)}u_{h,1}^i + \overline{\mu_h}, \tag{33}$$

for $i=1,...,N$. Steps 2 and 3 compute unnormalised and normalised weights for all particles, respectively.

At time $t>1$, Step 1 sorts the particles from smallest to largest and obtains the sorted particles and weights. Step 2 in Algorithm 4 resamples the particles using multinomial resampling and obtain the ancestor index $a_{t-1}^{1:N}$ in the original order of the particles in Step 3. Step 4 generates

$$h_t^i = \overline{\mu_h} + \phi\left(h_{t-1}^{a_{t-1}^i} - \overline{\mu_h}\right) + \rho\tau\exp\left(-\frac{h_{t-1}^{a_{t-1}^i}}{2}\right)(y_{t-1}-\phi_y y_{t-2}) + \sqrt{\tau^2(1-\rho^2)}u_{h,t}^i, \tag{34}$$

for $i=1,...,N$; it then compute the unnormalised and normalised weights of all particles.

**Algorithm 3** The Correlated particle filter (CPF) algorithm

Input: $u_{h,1:T}^{1:N}$, $u_{A,1:T-1}^{1:N}$, and $N$
Output: $h_{1:T}^{1:N}$, $a_{1:T-1}^{1:N}$, and $\overline{w}_{1:T}^{1:N}$
For $t=1$,

1. Set $h_1^i = H\left(u_{h,1}^i;\theta\right)$ for $i=1,...,N$.
2. Compute the unnormalised weights $w_1^i$, for $i=1,...,N$.
3. Compute the normalised weights $\overline{w}_1^i$ for $i=1,...N$.

For $t\geq 2$

1. Sort the particles $h_{t-1}^i$ from the smallest to largest and obtain the sorted indices $\zeta_i$ for $i=1,...,N$, and the sorted particles and weights $\widetilde{h}_{t-1}^i = h_{t-1}^{\zeta_i}$ and $\widetilde{\overline{w}}_{t-1}^i = \overline{w}_{t-1}^{\zeta_i}$, for $i=1,\ldots,N$.
2. Obtain the ancestor indices based on the sorted particles $\widetilde{a}_{t-1}^{1:N}$ using the multinomial resampling in Algorithm 4.
3. Obtain the ancestor indices based on the original order of the particles $a_{t-1}^i$ for $i=1,...,N$.
4. Set $h_t^i = H\left(u_{ht}^i;\theta,h_{t-1}^{a_{t-1}^i}\right)$, for $i=1,...,N$.
5. Compute the unnormalised weights $w_t^i$, for $i=1,...,N$
6. Compute the normalised weights $\overline{w}_t^i$ for $i=1,...,N$

**Algorithm 4** Multinomial Resampling Algorithm

Input: $u_{A,t-1}$, sorted particles $\widetilde{h}_{t-1}^{1:N}$, and sorted weights $\widetilde{\widetilde{w}}_{t-1}^{1:N}$ (see Algorithm 3) Output: $\widetilde{a}_{t-1}^{1:N}$

1. Compute the cumulative weights

$$\widehat{F}_{t-1}^{N}(j) = \sum_{i=1}^{j} \widetilde{\widetilde{w}}_{t-1}^{i}.$$

based on the sorted particles $\left\{\widetilde{h}_{t-1}^{1:N}, \widetilde{\widetilde{w}}_{t-1}^{1:N}\right\}$

2. Set $\widetilde{a}_{t-1}^{i} = \min_{j} \quad \widehat{F}_{t-1}^{N}(j) \geq u_{A,t-1}^{i}$ for $i = 1, ...N$; For $i = 1, ..., N$; $\widetilde{a}_{t-1}^{i}$ is the ancestor index based on the sorted particles.

# D Impulse responses for macroeconomic variables (baseline)

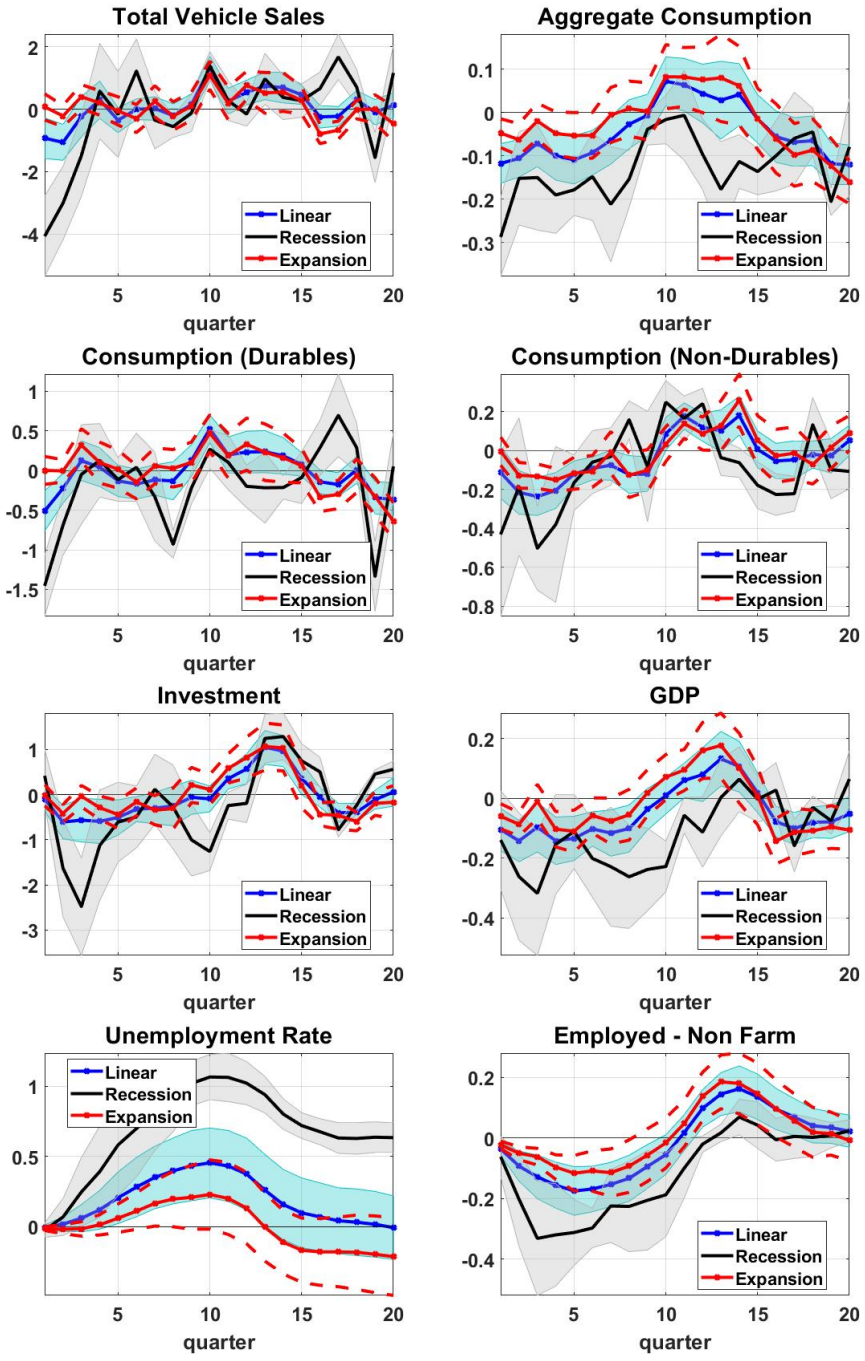


**Figure 14:** Impact of changes in $\eta_t^*$ on real activity. Impulse responses calculated for the quarterly real growth rate of total vehicle sales, durable consumption, total consumption, non-durable consumption, investment, GDP, the unemployment rate and total employed in the non-farm sector. The blue line is the effect of a one standard deviation shock to $\eta_t^*$ in the linear model (shaded blue area – 68% CI). The black line is the effect of a one standard deviation shock to $\eta_t^*$ in recessions (shaded gray area – 68% CI). The red line is the effect of a one standard deviation shock to $\eta_t^*$ in expansions (dashed red line – 68% CI).

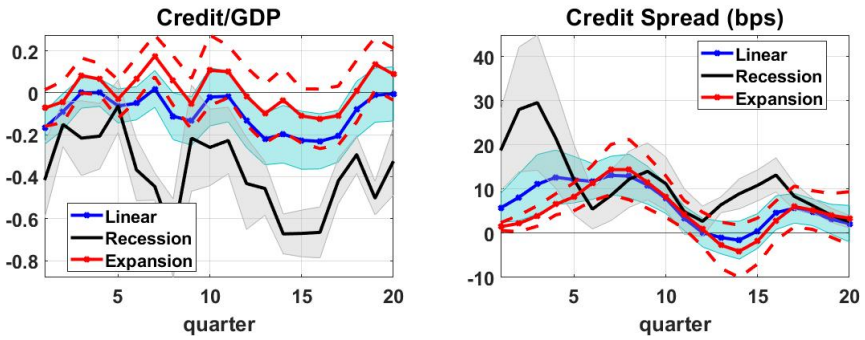


**Figure 15:** Impact of changes in $\eta_t^*$ on credit markets. Impulse responses calculated for household leverage (household credit/GDP), and the credit spread computed as the difference between the Baa and Aaa bonds. The black line is the effect of a one standard deviation shock to $\eta_t^*$ in recessions (shaded gray area – 68% CI). The red line is the effect of a one standard deviation shock to $\eta_t^*$ in expansions (dashed red line – 68% CI).

# E Impulse responses with shocks constructed using data on Consumer Credit

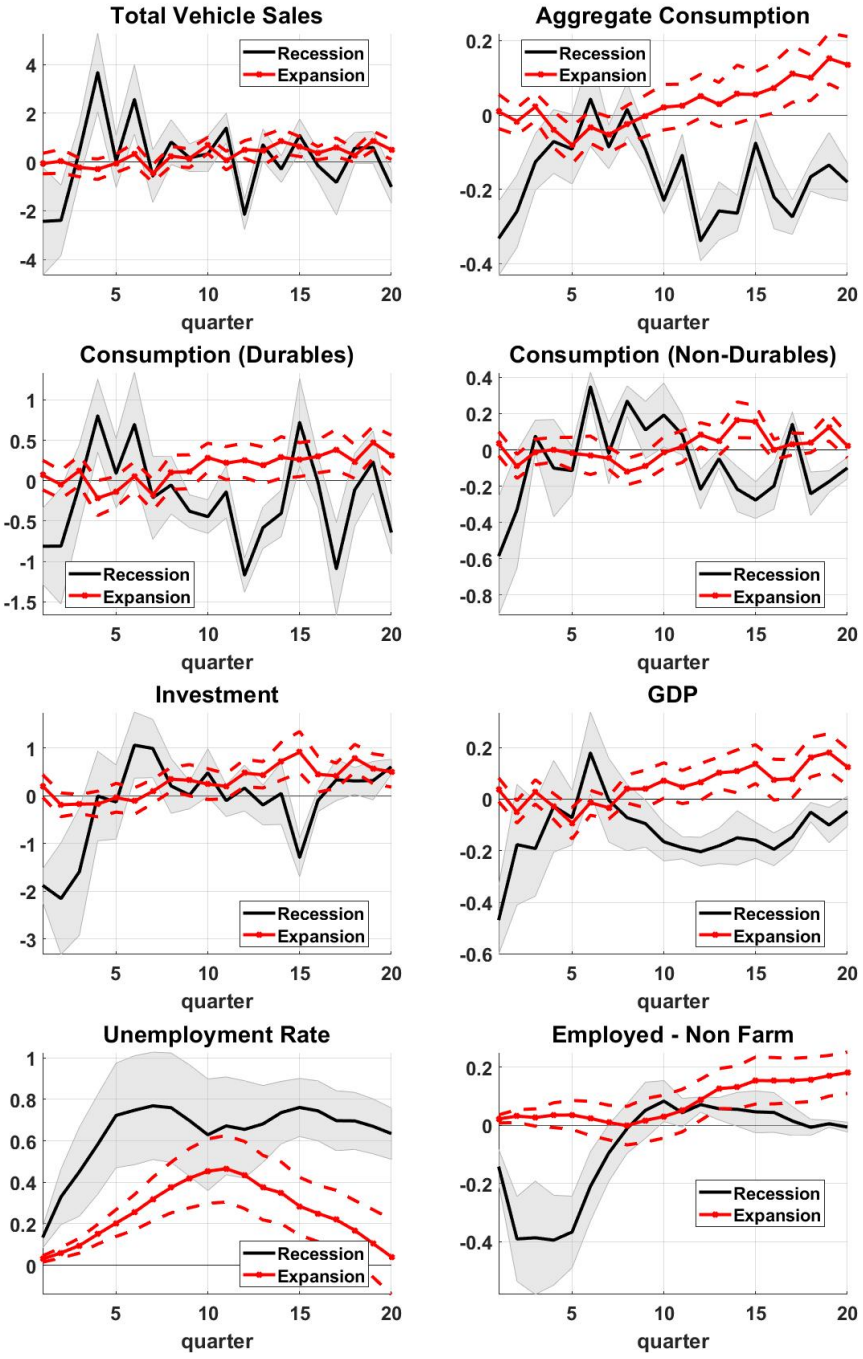


**Figure 16:** Impact of changes in $\eta_t^*$ on real activity. Impulse responses calculated for the quarterly real growth rate of total vehicle sales aggregate consumption, expenditure on durable consumption, expenditure on non-durable consumption, investment and the unemployment rate. The black line is the effect of a one standard deviation shock to $\eta_t^*$ in recessions (shaded gray area – 68% CI). The red line is the effect of a one standard deviation shock to $\eta_t^*$ in expansions (dashed red line – 68% CI).

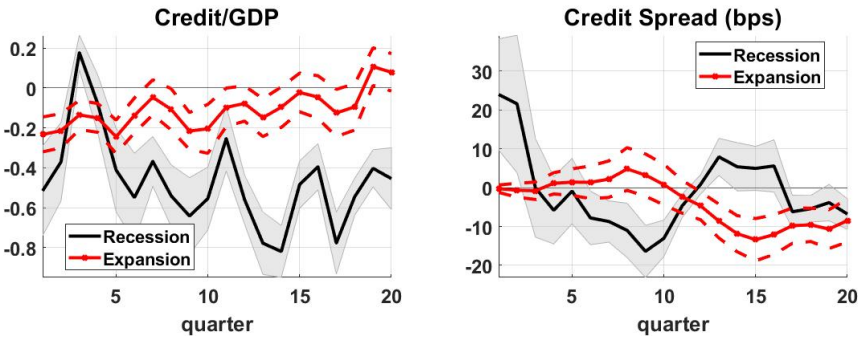


**Figure 17:** Impact of changes in $\eta_t^*$ on credit markets. Impulse responses calculated for the growth rate of household leverage (household credit/GDP) and the difference between Baa and Aaa corporate bond yields. The black line is the effect of a one standard deviation shock to $\eta_t^*$ in recessions (shaded gray area – 68% CI). The red line is the effect of a one standard deviation shock to $\eta_t^*$ in expansions (dashed red line – 68% CI).

# F Impulse responses with shocks constructed using data on Nonfinancial Business Debt


**Figure 18:** Impact of changes in $\eta_t^*$ on real activity. Impulse responses calculated for the quarterly real growth rate of total vehicle sales, durable consumption, total consumption, non-durable consumption, investment, GDP, the unemployment rate and total employed in the non-farm sector. The black line is the effect of a one standard deviation shock to $\eta_t^*$ in recessions (shaded gray area – 68% CI). The red line is the effect of a one standard deviation shock to $\eta_t^*$ in expansions (dashed red line – 68% CI).

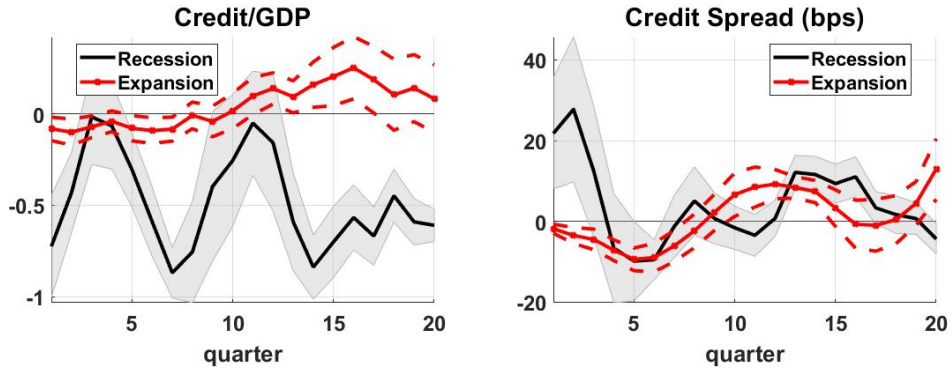


**Figure 19:** Impact of changes in $\eta_t^*$ on credit markets. Impulse responses calculated for the growth rate of household leverage (household credit/GDP) and the difference between Baa and Aaa corporate bond yields. The black line is the effect of a one standard deviation shock to $\eta_t^*$ in recessions (shaded gray area – 68% CI). The red line is the effect of a one standard deviation shock to $\eta_t^*$ in expansions (dashed red line – 68% CI).

# G Impulse responses for Net-Exports and U.S. Dollar Index

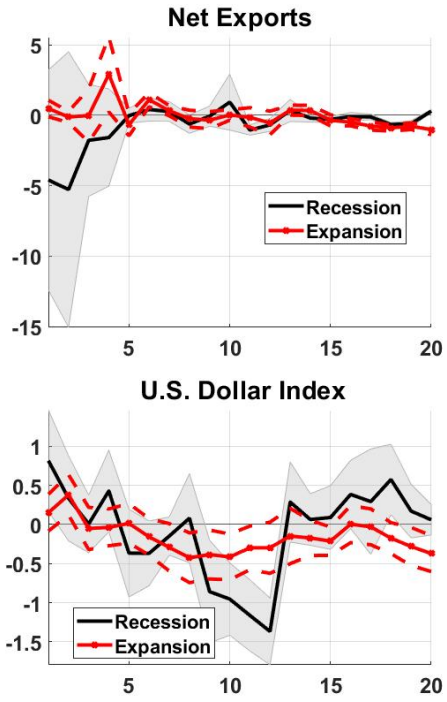


**Figure 20:** Impact of changes in $\eta_t^*$ on net-exports and the real exchange rate measured through the Broad Real Trade Weighted U.S. Dollar Index. The black line is the effect of a one standard deviation shock to $\eta_t^*$ in recessions (shaded gray area – 68% CI). The red line is the effect of a one standard deviation shock to $\eta_t^*$ in expansions (dashed red line – 68% CI).